MODELING OF VARIABLE COMPLIANT FOUR LEGGED ROBOT

A DISSERTATION

Submitted in partial fulfillment of the

requirements for the award of the degree
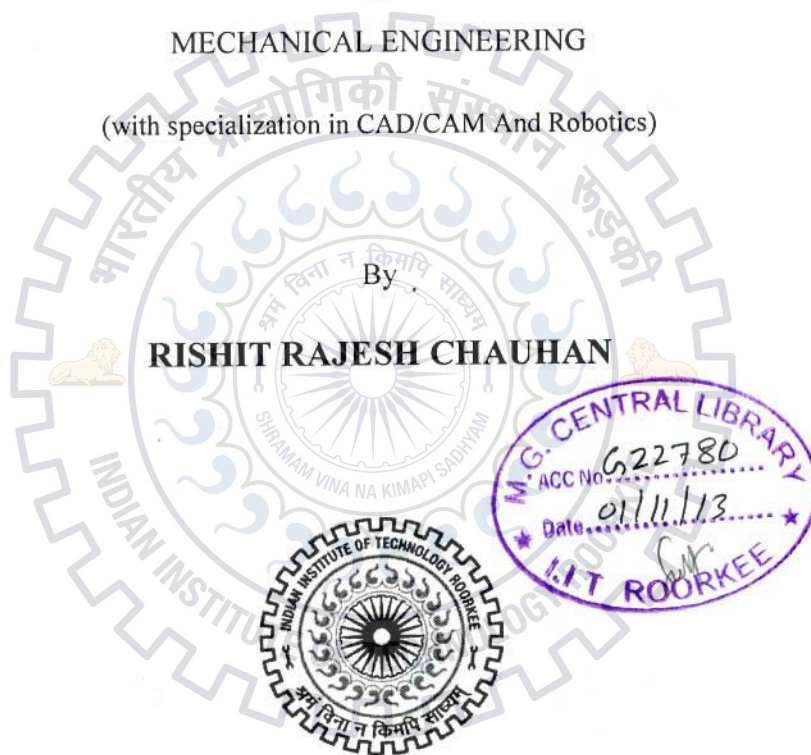
of

MASTER OF TECHNOLOGY

in

MECHANICAL ENGINEERING

(with specialization in CAD/CAM And Robotics)

By

RISHIT RAJESH CHAUHAN

DEPARTMENT OF MECHANICAL AND INDUSTRIAL ENGINEERING
INDIAN INSTITUTE OF TECHNOLOGY ROORKEE
ROORKEE-247 667 (INDIA)

JUNE, 2013

CANDIDATE'S DECLARATION

I hereby declare the work which is being presented in this dissertation entitled, **"MODELING OF VARIABLE COMPLIANT FOUR LEGGED ROBOT",** is presented on behalf of partial fulfillment for the award of degree of **Master of Technology** in Mechanical Engineering with specialization in **CAD/CAM and Robotics** submitted to the **Department of Mechanical and Industrial Engineering, Indian Institute of Technology, Roorkee** under the supervision of **Dr. P.M. Pathak**, Associate Professor, Department of Mechanical and Industrial Engineering.

I have not submitted the record embodied in this report for the award of any other degree or diploma.

Date: 10th June 2013

Place: Roorkee

RISHIT RAJESH CHAUHAN

CERTIFICATE

This is to certify that the above statement made by the candidate is correct to the best of my knowledge and belief.

Dr. P.M. PATHAK

Associate Professor

MIED

IIT ROORKEE

ACKNOWLEDGEMENT

I wish to express immense pleasure and sincere thanks to **Dr. P.M. Pathak**, Associate Professor, Department of Mechanical & Industrial Engineering, IIT Roorkee, for his valuable guidance and support. This work is simply the reflection of his thoughts, ideas and concepts and about his efforts. Working under his guidance was a privilege and an excellent learning experience that I will cherish for life time.

I also express my heartiest thanks to **Prof. P.K. Jain**, Head of Department of Mechanical & Industrial Engineering for his encouragement and overall supervision in bringing out this project report.

I am very thankful to my parents and all of my friends for their never ending encouragement in bringing out this seminar report to the form which it is in now.

<div align="right">
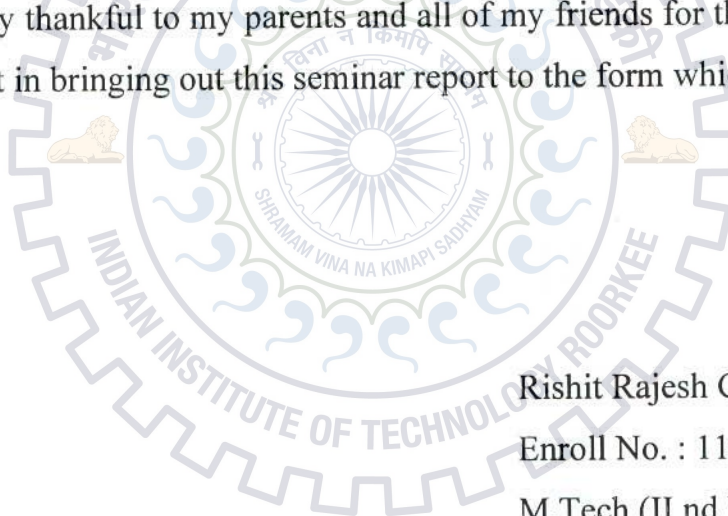
Rishit Rajesh Chauhan
Enroll No. : 11538002
M.Tech (II nd Year)
CAD/CAM & Robotics

</div>

Table Of Contents

LIST OF FIGURES

LIST OF TABLES

ABSTRACT

In the era of automation, the interaction of the humans with the robots is unavoidable. Hence, there is a need to improve the safety of humans that interact with the robots for the industrial as well as domestic purposes. Compliance in the body parts of the robot tends to provide safer human interactions. Compliance in the links also provides an energy efficient locomotion. Wheeled robots are limited in different types of terrain that they can navigate. In contrast, legged robots can navigate in a wide range of terrains. When compared to bipeds and hexapods, four legged walking robots provide a good trade off stability, load carrying capacity and mechanical complexity. Four legged robot is designed to travel in too steep, rutted rocky, wet muddy and snowy environment.

In this paper we propose a variable stiffness four legged robot. The bottom link of leg is C- shaped. There is a moving appendage which can slide over C- shaped link and thus changing the stiffness of the link. The physical mapping of the C- leg into a linear geometry is achieved using the SLIP (Spring Loaded Inverted Pendulum) model. The SLIP model is a well-established description of bouncy gaits. While in the original SLIP model leg parameters are fixed, in this paper, we include variations of rest length and linear stiffness. Dynamic model of the leg is created using Lagrange method. For the said analysis, the dynamic model of the robot is simulated in MATLAB by assuming initial values of the masses of legs, friction, impact force and inclined ground surface. The modeling of the robot is carried out in sagittal plane and bounding gait has been considered for the simulation purposes. The dynamic model achieved can be further used for designing the controller.

1.1 Introduction

Legged robots can move on different types of surfaces while wheeled robots are limited in the choice of surfaces that they can navigate. When compared to Bipeds and Hexapods, Four legged walking robots display better stability, load carrying capacity and mechanical complexity. In order to achieve optimum mobility, dynamic walking and running operation is preferable to static gaits. This, in turn requires leg compliance to reduce impact force and energy consumption. On earth animals and humans use legged locomotion because of the incredible adaptability and versatility this method of locomotion provides. It has the ability to travel in all kinds of terrain. It can move on rough, uneven, smooth terrains and also used to climb stairs and get passed obstacles whereas wheeled robots are limited. Legged robots can travel with less ground-robot contact as compared to wheeled or tracked vehicles, which require continuous contact. On flat terrain, wheeled locomotion is faster and more efficient than legged locomotion however it fails to function adequately in areas where the terrain is not level. Legged locomotion has the ability to reach places that wheeled locomotion cannot.

In order to overcome some of the limitations of wheeled or tracked vehicles, a number of hybrid vehicles, combining legs, wheels and articulated tracked vehicles have been developed. Such devices are able to achieve greatly improved mobility and are increasingly used in the areas of bomb disposal, construction, excavation and forestry in rough terrain, military tasks, and others.For legged robots to achieve practical utility, they must become faster, more forceful, more proficient, more independent and cheaper than contemporary prototypes. On that account dynamically stable machines are the best alternative.

Static machines are constrained by limited achievable speeds and must have a high number of legs and actuators, which makes them expensive and complex to control. For a Statically stable robot it is imperative to have at least four legs to maintain static stability, or it could also typically have six or eight to provide sufficient mobility over rough terrain. On the other hand, dynamically stable robots can operate with relatively fewer legs, some even on just one. This makes the design simpler, permits higher speeds and displays a wider number of behaviours.

Historically, one of the main reasons for introducing robots to industry was to eliminate human operators from working in a possible hazardous environment. Ironically, very often the robots were a potential threat to the workers. Industrial robots are designed and controlled with the idea to optimize performance, thus providing them with a high speed of execution, high accuracy and high repeatability. Their high weight, high speed, stiff characteristics and high gain control make them dangerous if a collision with a human should occur. For this reason, people are not allowed in the vicinity of a robot while it is working.

In the last couple of years, the evolution in new and envisaged robotic applications involves a lot more close contact between humans and robots. There is a growing interest in robots that operate in close proximity to people, including physical interactions with them. There is a wide spectrum of possible applications that include rehabilitation robots (which help people relearn motor skills lost in an accident or due to stroke), robotic prosthesis, robot assistants for helping the elderly, manufacturing (with human-robot collaboration), entertainment robots, wearable robots, etc. The requirements for the new generation of robots are numerous and different.

Unlike industrial robots, they function in an unstructured environment, and have only partial knowledge of their surroundings. Since contact between the robot and objects or people surrounding it is possible, safety is of utmost importance. In many applications of Robotics, such as, Industrial, Domestic, Military, etc., robots have to interface with their human counterparts in order to achieve more efficient and productive use of the Robots.

In classical robotic applications, actuators are required to be as stiff as possible to make precise position movements. These types of actuators are more suited for the precise position controlled applications. The Compliant actuators on the other hand, offer valuable advantages in certain novel applications, e.g., safe human-robot interaction, comfortable actuated prostheses, and orthoses, and in the design of legged robots. Hence, the future of robotics lies in the design and development of compliant actuators that can be used in mobile robots requiring human interaction.

1.2 Literature Review

In the last couple of years, a great deal of research has been carried out in the area of dynamically stable robots. The first dynamically stable robot was the BIPER, which was built by **Miura and Shimoyama [1]**. This was a biped robot controlled by three motors that

could achieve dynamically stable walking. **Raibert [2]** initiated a more detailed research on dynamically stable robots by working on simple controllers for his pneumatic monopod. He introduced simple running control concepts such as the three part running controller - one each for hopping height, forward speed and body pitch – that were simple yet effective. He further expanded the scope of his work to bipeds and quadrupeds.

On researching further into running the advantages of passive elements in the robots were found. The concept of passive walking and running with biped robots was studied by **McGeer [3]**. He researched passive-dynamic running with legged robots having passive hip actuators and linear springs along the leg length. McGeer showed that running can be accomplished without any force required to generate the gait, through analytical work and simulation.

More work on legged robots with actuated and unactuated degrees of freedom such as, Scout II include investigation into ankle compliance. Control strategies for such a mechanism have been attempted by **Keon [4]**. He suggested a controller for a biped with two degrees of freedom actuated hip and two degrees of freedom compliance in the ankle. His simulation results proved that such a mechanism works very effectively.

Kimura et al. [5] introduced a quadruped running robot that has an actuated hip and knee joints as well as a passive spring mechanism for each leg. The running controller is based on a neural oscillator network, a stretch reflex as well as a flexor reflex mechanism. With this approach dynamic running and walking on flat terrain was successfully accomplished.

Furusho et al. [6] implemented a bounding gait on the SCAMPER robot. Even though the robot was not designed with explicit mechanical compliance, the compliance of the feet, legs, the belt transmission and the effective compliance of the PD joint servo loops are likely significant. The controller divided each complete running cycle into eight states and switched the two joints per leg between free rotation, position control and velocity control.

Berkemeier [7] performed an analytical study on a simplified quadrupedal running robot. Although expressions for exact maps could not be obtained, approximate maps for bounding and pronking were derived and used to predict the behaviour of the different running parameters. The simple model predicted that, for a given set of parameters, the bound offers greater acceleration since its period is shorter, and so the legs contact the ground more frequently. This also allows a greater manoeuvrability since it gives more

3

opportunities to steer around obstacles. The bounding gait is the main type of running that is addressed in this study.

In the year 2009, **Souto et al. [8]** made a four legged walking robot. Each leg had three links connected with rotational joints and a one end effector, thus forming a kinematic chain. They derived a kinematic model for the above quadruped robot. The model was similar to that of a parallel robot, in that each leg was seen as a robot. This model was extended such that, during one gait cycle some legs were in contact with the ground and others were not. In gait cycle swing legs followed sinusoid like trajectory where as supporting legs followed straight line trajectory. In order to obtain the inverse kinematics model, they used the extended Kalman filter as optimizer in two different situations of the leg motion: unconstrained case, for the swing leg(s), and constrained case, for the leg(s) in contact with the ground.

In 1996, **Ahmadi and Buehler [9]** made a control strategy for a one legged running robot with compliant elements connected in series with hip and leg actuators. They derived dynamic equations of motion for both stance and flight phase. They selected proper spring and initial conditions that resulted in passive dynamic operations which were closer to the desired motion without any actuation.

In the year 2000, **Papadopoulos and Buehler [10]** studied a four legged walking robot named Scout II with hip actuator and an additional compliant prismatic joint for each leg. They derived equations of motion of Scout II during running phase. Then they integrated the equation of motion for the different running phases and then plotted data for the state variables such as body pitch, body pitch speed, leg angles, leg angular speeds, leg length and leg length speed against time. In order to verify the Scout II mathematical model, they made the Scout II model a working model 2D package and simulated it. State variables obtained from both the working model 2D package and the mathematical model were simulated in MATLAB and compared.

In the year 2004, **Cherouvim and Papadopoulos [11]** explored the mechanism of energy transfer between the single actuated degrees of freedom (DOF) of a one-legged hopping robot and the remaining unactuated DOFs, during stable running. They considered two distinct models. The first model developed corresponds to a realistic robot incorporating a pitching body, inertia in the leg, as well as friction both at the hip and the leg. This model is referred to as the full model. The second one is the slip (SLIP) model, with a point mass as body, no body pitching and a mass-less leg. They derived equations of motion for both stance and flight phases.

4

In 2004, **Papadopoulos and Cherouvim [12]** made a study on one-legged hopping robot. A particular passive gait is available of all those possible, for which the dissipated energy per meter of travel is minimized. An analytical method was used to identify the optimal gait. The dynamics of the robot were approximated by a slip (SLIP) model. Certain assumptions were made to come to an analytical prediction for the optimal gait. Both mechanical and electrical losses were taken into account. A numerical analysis of a complete robot model was used to evaluate the accuracy of the analytical prediction. The analytical prediction found was fairly accurate, and had a simple form that correctly predicts the qualitative behaviour of all the parameters involved. Also, the accuracy of the analytical prediction had been verified with simulations of a complete robot model, including pitching of the body mass, as well as inertia in the leg. Finally, a model of a torque-limited actuator was included in the model. The analysis predicts which gaits are possible and whether the optimal gait can be achieved with a given motor.

In year 2008, **Scarfogliero et al. [13]** presented the design of a miniature jumping robot. Inspired by small jumping animals, the robot performs catapult jumps, using elastic energy storage and a release mechanism. Compliant forelegs were completely passive, and cushion the landing reusing part of the impact energy. Starting from the study of scaling effects in locomotion, a jumping gait for small legged robots has been investigated. The design of the jumping robot "Grillo" was suggested by jumping frogs, leading to elastic energy storage in order to increase the peak power output with respect to the mean motor power. Passive forelegs cushion used for landing impact and avoid rebounding. They presented a method to dimension compliant joints that affect any kind of locomotion for effective design optimizing of elastic energy storage and compliancy for a jumping gait.

In year 2009, **Radkhah et al. [14]** designed a biologically inspired compliant Four-Legged Robot. They summarized some basic principles of legged locomotion in animals and discussed the application of the principles to the design and fabrication of a four legged robot. Their model combined ideas for better locomotion of robots both in the biologically inspired, mechanically intelligent structure and in the bionic controller. Two novel features of our four-legged concept comprised the possibility of easily changing the spring stiffness deployed in the bionic drives of the joints and the way of this adjustment which required neither complex computation nor additional motor. By changing the controller parameters it is possible to let the model walk various gaits. The results of the optimization of the segments lengths demonstrate quite impressively that the extracted data from natural

5

archetypes can directly be taken over or used as good starting values for the optimization process.

In 2012, **M.M. Ankarali et al [15]** presented a simple dynamic model for the C-Leg design for a planar monopod, taking into account both the kinematics of rolling contact and the nonlinear compliance of the geometry. They showed through simulations that realistic predictions for the system trajectories can be generated and left the experimental validation of this model for future work.

Kevin C. Galloway et al [16]suggested that variable stiffness C- legs for dynamic locomotion of a RHex robot are a key control parameter in responding to changes in running gait, payload and terrain. In that paper, they had presented the design and construction of a structurally controlled stiffness limb which utilizes a single degree of freedom mechanism to control, in three dimensions, the stiffness properties of the leg.

Jonathan E. Clark et al [17]developed a robust, self-locking, structure-controlled, tunable stiffness leg for implementation on a dynamic hexapedal robot. They had shown that with a proper selection of materials and geometries, the proposed tunable leg can achieve a factor of 2or more change in stiffness without a significant change in deflection behavior. Several materials have been considered; however, we have found that composite materials offer the best combination of energy storage capacity, high yield strength, ease of manufacturing, and Young's modulus control.

K. Ganesh and Dr. P.M. Pathak [18] simulated and animated a four legged robot with compliant legs in a sagittal plane. They also used PD control algorithm to control the forward speed. A simulation model implementation is also created using the specified algorithm.

1.3   Contribution of the Thesis

This thesis deals with the contribution towards the Four Legged Robots.

Dynamic modeling – Dynamic modeling of four legged robot with C- links at the bottom has been derived. In this various factors such as, masses of legs and body, friction, impact force and inclined ground surface have been considered. The equations of motion of the system have been derived for the different running phases of bounding gait.

Simulink modeling – Simulink modeling for the bounding gait has been modeled and simulated in MATLAB/SIMULINK.

6

Animation – Animation of the working model has been done by extracting the planar co-ordinates of every joints of the robot and using these co-ordinates the robot has been animated in SYMBOLS SHAKTI Animator.

1.4 Overview of the Thesis

In chapter 2, the equations of motion for the different phases of the four legged walking robot with C-links at the bottom are derived. It gives the mathematical model corresponding to the physical system.

In chapter 3 Simulink modeling for the equations of motion are made and its results are discussed. In this all the equations are integrated and bounding gait is formed. Data plots of the various parameters are shown.

In Chapter 4, Animation models' snapshots are shown. They give the clear idea of how the robot is running.
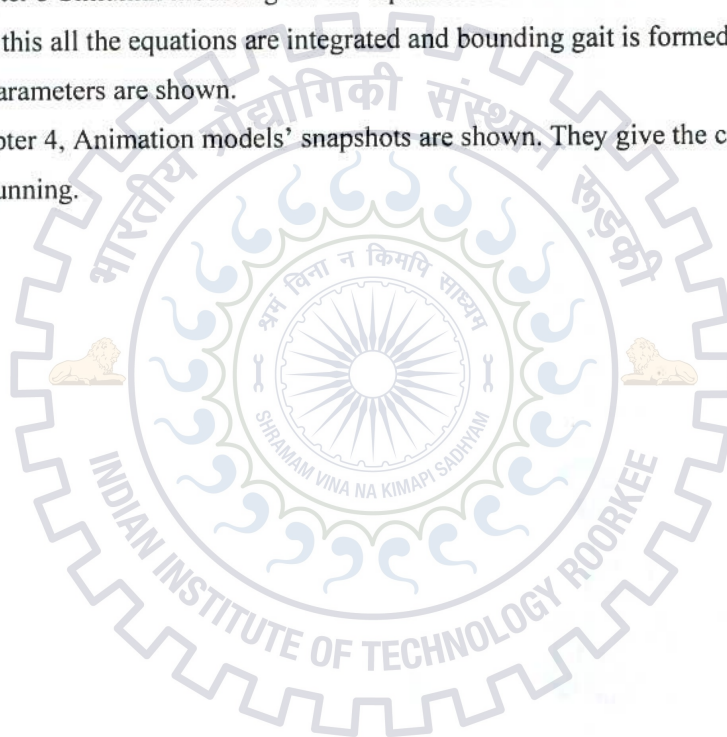
CHAPTER 2   MODELING OF A FOUR LEGGED ROBOT WITH VARIABLE COMPLIANT C-LEGS

In this chapter dynamic equations of motion are derived for all the stance phases using Lagrange method. These equations of motion play a vital role in modeling og the robot.

For computational ease,

2.1 Definitions

Running is defined by a sequence of dynamically stable events whereby the robot alternates between stance and flight phases. Stance occurs when any of the robot's legs are in contact with the ground, while flight occurs when all of the legs are in the air. In order for the robot to get around from one location to another, repetitive cycles of stance and flight states must take place. To achieve running, a quadruped can use a number of leg sequences. Each set of sequences is called a gait. In the bounding gait, the front legs move together, and so do the hind legs.

One complete cycle of bounding gait can be divided into four states, as shown in Fig.2.1. The state of the robot in each of the four events is as follows:
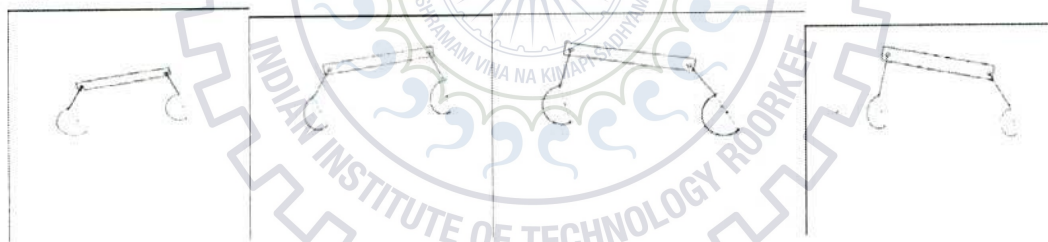
Figure 2.1: Different Stances of Four Legged Robot

The definitions of the various stances for the bounding gait are as follows:

> *Back stance:* This is the configuration where the robot is supported on the ground by its back legs.

> *Flight after back stance:* This is the configuration where none of the robot legs are touching the ground and the robot has just left the ground after a back stance.

> *Front stance:* This is the configuration where the robot is supported on the ground by its front legs.

8

> ➤ *Flight after front stance:* This is the configuration where none of the robot legs
> are touching the ground and the robot has just left the ground after a front stance.

2.2 Back Stance
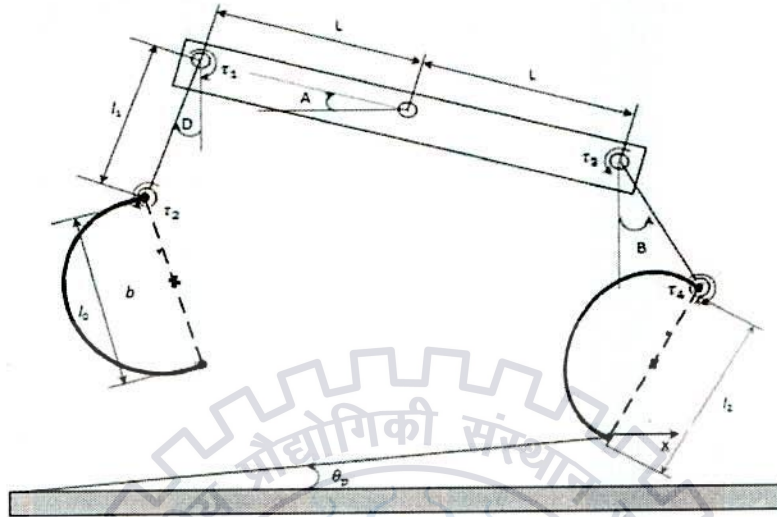
Figure 1.2: Back Stance Configuration

where,

$$A = \theta - \theta_p$$

$$B = \theta_3 - \theta + \theta_p$$

$$C = \psi = \theta_4 - \theta_3 + \theta - \theta_p$$

$$D = \theta - \theta_p + \theta_1$$

$$E = \theta_2 - \theta_1 - \theta + \theta_p$$

Fig 2 shows the back stance phase model of quadrupeds. The generalized coordinate vector q for this system is chosen to be $q = [\psi, \theta, \theta_1 \theta_2]^T$. From the generalized coordinates and Figure, the dynamics equations of motion can be derived as follows,

9

Cartesian coordinates for body

The body Cartesian coordinates can be expressed at the contact point of the back leg's toe and the ground as follows,

$$[P_{bb}] = \begin{vmatrix} L\cos(\theta + \theta_p) + l_1\sin(\theta_1 - (\theta + \theta_p)) - 2r_l\cos(\psi)\sin(\theta_2 - \theta_1 + (\theta + \theta_p)) \\ L\sin(\theta + \theta_p) + l_1\cos(\theta_1 - (\theta + \theta_p)) + 2r_l\cos(\psi)\cos(\theta_2 - \theta_1 + (\theta + \theta_p)) \end{vmatrix}$$

These can be differentiated with respect to time, in order to give the body velocities in the x- and y- directions,

$$[\dot{P}_{bb}] = \begin{bmatrix} -L\dot{\theta}\sin(\theta + \theta_p) + l_1(\dot{\theta}_1 - \dot{\theta})\cos(\theta_1 - (\theta + \theta_p)) - 2r_l\cos(\psi)(\dot{\theta}_2 - \dot{\theta}_1 + \dot{\theta}) \\ \cos(\theta_2 - \theta_1 + (\theta + \theta_p)) - 2r_l(\dot{\psi})\sin(\psi)\sin(\theta_2 - \theta_1 + (\theta + \theta_p)) \\ L\dot{\theta}\cos(\theta + \theta_p) - l_1(\dot{\theta}_1 - \dot{\theta})\sin(\theta_1 - (\theta + \theta_p)) - 2r_l\cos(\psi)(\dot{\theta} + \dot{\theta}_2 - \dot{\theta}_1) \\ \sin(\theta_2 - \theta_1 + (\theta + \theta_p)) + 2r_l(\dot{\psi})\sin(\psi)\cos(\theta_2 - \theta_1 + (\theta + \theta_p)) \end{bmatrix}$$

Kinetic Energy of the body can be expressed as,

$$T_{bb} = \frac{1}{2}m\left(L^2\dot{\theta}^2 + l_1{}^2(\dot{\theta}_1 - \dot{\theta})^2 + l_2{}^2(\dot{\theta} + \dot{\theta}_2 - \dot{\theta}_1)^2 + \dot{l}_2{}^2 + r_b{}^2\dot{\theta}^2 + 2[-Ll_1\dot{\theta}(\dot{\theta}_1 - \dot{\theta})\sin(\theta_1) + Ll_2\dot{\theta}(\dot{\theta} + \dot{\theta}_2 - \dot{\theta}_1)\sin(\theta_1 - \theta_2) + L\dot{l}_2\dot{\theta}\cos(\theta_1 - \theta_2) - l_1l_2(\dot{\theta}_1 - \dot{\theta})(\dot{\theta} + \dot{\theta}_2 - \dot{\theta}_1)\cos(\theta_2) - l_1\dot{l}_2(\dot{\theta}_1 - \dot{\theta})\sin(\theta_2)]\right)$$

Potential Energy of the body,

$$V_{bb} = m_b g\left[L\sin(\theta + \theta_p) + l_1\cos(\theta_1 - (\theta + \theta_p)) + l_2\cos(\theta_2 - \theta_1 + (\theta + \theta_p))\right]$$

Back leg , Link 1,

Kinetic Energy,

$$T_{b1b} = \frac{1}{2}m_1\left[l_2{}^2(\dot{\theta} + \dot{\theta}_2 - \dot{\theta}_1)^2 + \dot{l}_2{}^2 + r_{b1}{}^2\dot{\theta}_1{}^2\right]$$

Potential Energy,

$$V_{b1b} = m_1 g\left[l_2\cos(\theta_2 - \theta_1 + \theta + \theta_p)\right]$$

Back leg, Link2 (C-link),

Kinetic Energy can be expressed as,

$$T_{b2b} = \frac{1}{2} m_2 r_{b2}^2 \dot{\theta}^2$$

Potential Energy can be expressed as,

$$V_{b2b} = \frac{1}{2} k \cos(\text{constant}(\psi + \psi_0))(4r_l^2 \cos^2(\psi + \psi_0) - l_0)^2$$

Front leg, Link1,

Cartesian coordinates for the link1 can be expressed as,

$$[P_{f1b}] = \begin{vmatrix} 2L\cos(\theta + \theta_p) + l_1\sin(\theta_1 - (\theta + \theta_p)) - 2r_l\cos(\psi)\sin(\theta_2 - \theta_1 + (\theta + \theta_p)) \\ +l_1\sin(\theta_3 + \theta + \theta_p) \\ 2L\sin(\theta + \theta_p) + l_1\cos(\theta_1 - (\theta + \theta_p)) + 2r_l\cos(\psi)\cos(\theta_2 - \theta_1 + (\theta + \theta_p)) \\ -l_1\cos(\theta_3 + \theta + \theta_p) \end{vmatrix}$$

By differentiating these coordinates the velocities in the x-directions and y-directions can be written as,

$$[\dot{P}_{f1b}] =$$

$$\begin{bmatrix} -2L\dot{\theta}\sin(\theta + \theta_p) + l_1(\dot{\theta}_1 - \dot{\theta})\cos(\theta_1 - (\theta + \theta_p)) - 2r_l\cos(\psi)(\dot{\theta} + \dot{\theta}_2 - \dot{\theta}_1) \\ \cos(\theta_2 - \theta_1 + \theta + \theta_p) - 2\dot{r}_l\dot{\psi}\sin(\psi)\sin(\theta_2 - \theta_1 + \theta + \theta_p) + l_1\dot{\theta}\cos(\theta_3 + \theta + \theta_p) \\ 2L\dot{\theta}\cos(\theta + \theta_p) - l_1(\dot{\theta}_1 - \dot{\theta})\sin(\theta_1 - (\theta + \theta_p)) - 2r_l\cos(\psi)(\dot{\theta} + \dot{\theta}_2 - \dot{\theta}_1) \\ \sin(\theta_2 - \theta_1 + \theta + \theta_p) - 2\dot{r}_l\dot{\psi}\sin(\psi)\cos(\theta_2 - \theta_1 + \theta + \theta_p) + l_1\dot{\theta}\sin(\theta_3 + \theta + \theta_p) \end{bmatrix}$$

Kinetic Energy,

$$T_{f1b} =$$

$$\frac{1}{2}m_1\left[4L^2\dot{\theta}^2 + l_1^2(\dot{\theta}_1 - \dot{\theta})^2 + 4r_l^2\cos^2(\psi + \psi_0)(\dot{\theta} + \dot{\theta}_2 - \dot{\theta}_1)^2 + 4r_l^2\dot{\psi}\sin(\psi) + \right.$$

$$l_1^2\dot{\theta}^2 + 2[-2Ll_1\dot{\theta}(\dot{\theta}_1 - \dot{\theta})\sin(\theta_1) + 2L2r_l\cos(\psi)\dot{\theta}(\dot{\theta} + \dot{\theta}_2 - \dot{\theta}_1)\sin(\theta_1 - \theta_2) +$$

$$2L2r_l\dot{\psi}\sin(\psi)\dot{\theta}\cos(\theta_1 - \theta_2) - 2Ll_1\dot{\theta}^2\sin(\theta_3) - l_12r_l\cos(\psi)(\dot{\theta}_1 - \dot{\theta})(\dot{\theta} + \dot{\theta}_2 -$$

$$\dot{\theta}_1)\cos(\theta_2) - l_12r_l\dot{\psi}\sin(\psi)(\dot{\theta}_1 - \dot{\theta})\sin(\theta_2) + l_1^2(\dot{\theta}_1 - \dot{\theta})\dot{\theta}\cos(\theta_1 + \theta_3) +$$

$$\left. l_12r_l\dot{\psi}\sin(\psi)\dot{\theta}\sin(\theta_3 + \theta_1 - \theta_2) - l_12r_l\cos(\psi)(\dot{\theta} + \dot{\theta}_2 - \dot{\theta}_1)\dot{\theta}\cos(\theta_3 + \theta_1 - \theta_2)]\right]$$

Potential Energy,

$$V_{f1b}=m_1g\left[2L\sin(\theta+\theta_p)+l_1\cos(\theta_1-(\theta+\theta_p))+2r_l\cos(\psi)\cos(\theta_2-\theta_1+\theta+\theta_p)-l_1\cos(\theta_3+\theta+\theta_p)\right]$$

Front Leg, Link 2 (C-Link)

Kinetic Energy can be expressed as,

$$
\begin{aligned}
T_{b2f} = \frac{1}{2}m_2\Big\{ & 4L^2\dot{\theta}^2 + l_1^2\left(\dot{\theta}_1-\dot{\theta}\right)^2 + 4r_l^2\cos^2(\psi)\left(\dot{\theta}+\dot{\theta}_2-\dot{\theta}_1\right)^2 + 4r_l^2\dot{\psi}^2\sin^2(\psi) \\
& + l_1^2\dot{\theta}^2 + 4r_l^2\dot{\psi}^2\sin^2(\psi)\dot{\theta}^2 \\
& + 2\Big[-2Ll_1\dot{\theta}(\dot{\theta}_1-\dot{\theta})\sin(\theta_1)+4Lr_l\cos(\psi)\dot{\theta}(\dot{\theta}+\dot{\theta}_2-\dot{\theta}_1)\sin(\theta_1-\theta_2) \\
& - 4Lr_l\dot{\psi}\sin(\psi)\dot{\theta}\cos(\theta_1-\theta_2)-2Ll_1\dot{\theta}^2\sin(\theta_3)-l_12r_l\cos(\psi)\left(\dot{\theta}_1-\dot{\theta}\right)(\dot{\theta} \\
& + \dot{\theta}_2-\dot{\theta}_1)\cos(\theta_2)+l_12r_l\dot{\psi}\sin(\psi)\left(\dot{\theta}_1-\dot{\theta}\right)\sin(\theta_2) \\
& + l_1^2\left(\dot{\theta}_1-\dot{\theta}\right)\dot{\theta}\cos(\theta_1+\theta_3)+l_12r_l\dot{\psi}\sin(\psi)\dot{\theta}\sin(\theta_3+\theta_1-\theta_2) \\
& - l_12r_l\cos(\psi)\left(\dot{\theta}+\dot{\theta}_2-\dot{\theta}_1\right)\dot{\theta}\cos(\theta_3+\theta_1-\theta_2)\Big]\Big\} \\
& + 2\Big[-4Lr_l\cos(\psi)\dot{\theta}^2\sin(\theta_4-\theta_3)+l_12r_l\cos(\psi)\left(\dot{\theta}_1-\dot{\theta}\right)\dot{\theta}\cos(\theta_1+\theta_3 \\
& - \theta_4)-2r_l^2\dot{\psi}\sin(2\psi)\dot{\theta}\sin(\theta_2-\theta_1-\theta_4+\theta_3) \\
& - 4r_l^2\cos^2(\psi)\dot{\theta}\left(\dot{\theta}+\dot{\theta}_2-\dot{\theta}_1\right)\cos(\theta_2-\theta_1+\theta_4-\theta_3) \\
& + l_12r_l\cos(\psi)\dot{\theta}^2\cos(\theta_4)\Big]
\end{aligned}
$$

Potential Energy can be expressed as,

$$V_{b2f} = m_2g\left[2L\sin(\theta+\theta_p)+l_1\cos(\theta_1-(\theta+\theta_p))+2r_l\cos(\psi)\cos(\theta_2-\theta_1+(\theta+\theta_p))-l_1\cos(\theta_3+\theta+\theta_p)-2r_l\cos(\psi)\cos(\theta_4-(\theta_3+\theta+\theta_p))\right]$$

Lagrangian Function

$$L =$$

$$
\frac{1}{2}\left[\begin{array}{c}\left[\dot{\theta}^2L^2(m_b+4m_1+4m_2)+\left(\dot{\theta}_1-\dot{\theta}\right)^2l_1^2(m_b+m_1+m_2)+4r_l^2\cos^2(\psi)\left(\dot{\theta}+\dot{\theta}_2-\dot{\theta}_1\right)^2\right]\\(m_b+2m_1+m_2)\\+4r_l^2\dot{\psi}^2\sin^2(\psi)(m_b+2m_1+m_2)+m_br_{bf}^2\dot{\theta}^2+m_1r_{f1}^2\dot{\theta}_1^2+m_2r_{f2}^2\dot{\theta}_2^2+l_1^2\dot{\theta}^2(m_1+m_2)+m_2l_0^2\dot{\theta}^2\end{array}\right]
$$

$$+(m_b+2m_1+2m_2)\left[Ll_1\dot{\theta}\left(\dot{\theta}-\dot{\theta}_1\right)\sin(\theta_1)\,2Lr_l\cos(\psi)\dot{\theta}\left(\dot{\theta}+\dot{\theta}_2-\dot{\theta}_1\right)\sin(\theta_1-\theta_2)+$$

$$2Lr_l\dot{\psi}\sin(\psi)\dot{\theta}\cos(\theta_1-\theta_2)\right]+$$

14

$$(m_b + m_1 + m_2)\left[2l_1 r_l \cos(\psi)\left(\dot\theta - \dot\theta_1\right)\left(\dot\theta + \dot\theta_2 - \dot\theta_1\right)\cos(\theta_2) + 2l_1 r_l \dot\psi \sin(\psi)\left(\dot\theta - \dot\theta_1\right)\sin(\theta_2)\right]$$

$$+(m_1 + m_2)\left[-2Ll_1\dot\theta^2 \sin(\theta_3) - l_1{}^2\left(\dot\theta - \dot\theta_1\right)\dot\theta\cos(\theta_1 + \theta_3) + 4l_1 r_l^2 \dot\psi^2 \sin^2(\psi)\dot\theta\sin(\theta_1 - \theta_2 + \theta_3) - 2l_1 r_l \cos(\psi)\left(\dot\theta + \dot\theta_2 - \dot\theta_1\right)\dot\theta\cos(\theta_1 - \theta_2 + \theta_3)\right]+$$

$$\left[\begin{array}{c} -4Lr_l\cos(\psi)\dot\theta^2\sin(\theta_4 - \theta_3) + l_1 2r_l\cos(\psi)\left(\dot\theta_1 - \dot\theta\right)\dot\theta\cos(\theta_1 + \theta_3 - \theta_4) \\ 2r_l^2\dot\psi\sin(2\psi)\dot\theta\sin(\theta_2 - \theta_1 + \theta_4 - \theta_3) - 4r_l^2\cos^2(\psi)\dot\theta\left(\dot\theta + \dot\theta_2 - \dot\theta_1\right)\cos(\theta_2 - \theta_1 + \theta_4 - \theta_3) \end{array}\right]$$
$$+2l_1 r_l\cos(\psi)\dot\theta^2\cos(\theta_4)$$

$$-g\left\{\begin{array}{c} (m_b + 2m_1 + 2m_2)L\sin(\theta + \theta_p) + (m_b + m_1 + m_2)l_1\cos(\theta_1 - (\theta + \theta_p)) \\ -(m_1 + m_2)l_1\cos(\theta_3 + \theta + \theta_p) - 2m_2 r_l\cos(\psi)\cos(\theta_4 - (\theta_3 + \theta + \theta_p)) \\ +(m_b + 2m_1 + m_2)2r_l\cos(\psi)\cos(\theta_2 - \theta_1 + \theta + \theta_p) \end{array}\right\}$$

$$-\frac{1}{2}k\cos(constant(\psi + \psi_0))(2r_l\cos(\psi) - l_0)^2$$

Equation of motion for generalized coordinate ψ

By direct substitution of equation (2.28) in the below equation, the equation of motion for generalised coordinate ψ can be calculated

$$\frac{d}{dt}\left(\frac{DL}{D\dot\psi}\right) - \frac{DL}{D\psi} + \frac{DB}{D\psi} = F$$

The equation of motion for generalised Coordinate l_2 becomes,

$$-2(m_b + 2m_1 + m_2)r_l\dot\psi^2\cos(\psi) + [(m_b + 2m_1 + 2m_2)L\cos(\theta_1 - \theta_2) + (m_b + m_1 + m_2)l_1\sin(\theta_2) + (m_1 + m_2)l_1\sin(\theta_1 - \theta_2 + \theta_3) - 2m_2 r_l\cos(\psi)\sin(\theta_2 - \theta_1 + \theta_4 - \theta_3)]\ddot\theta$$

$$-[(m_b + m_1 + m_2)l_1\sin(\theta_2)]\ddot\theta_1 - [(m_b + 2m_1 + m_2)]l_2\left(\dot\theta + \dot\theta_2 - \dot\theta_1\right)^2$$

$$-(m_b + 2m_1 + 2m_2)L\dot\theta^2\sin(\theta_1 - \theta_2) - (m_b + m_1 + m_2)l_1\left(\dot\theta - \dot\theta_1\right)^2\cos(\theta_2) + (m_1 + m_2)l_1\dot\theta^2\cos(\theta_1 - \theta_2 + \theta_3) + 2m_2 r_l\cos(\psi)\dot\theta^2\cos(\theta_2 - \theta_1 + \theta_4 - \theta_3) + g(m_b + 2m_1 + m_2)\cos(\theta_2 - \theta_1 + \theta + \theta_p) + k\cos(constant(\psi + \psi_0))(l_0 - 2r_l\cos(\psi)) =$$

$$F_i\cos(\theta_2 - \theta_1 + \theta + \theta_p) + \mu F_i\cos(\theta_2 - \theta_1 + \theta + \theta_p)$$

Equation of motion for generalized coordinate θ

By direct substitution of equation (2.28) in the below equation, the equation of motion for generalised coordinate θ can be calculated

$$\frac{d}{dt}\left(\frac{DL}{D\dot{\theta}}\right) - \frac{DL}{D\theta} + \frac{DB}{D\dot{\theta}} = 0$$

The equation of motion for generalised Coordinate θ becomes,

$-[(m_b+2m_1+2m_2)\, L\cos(\theta_1-\theta_2) + (m_b+m_1+m_2)\, l_1\sin(\theta_2)+ (m_1+m_2)\, l_1\sin(\theta_3+\theta_1-\theta_2) - 2m_2\, r_l\cos(\psi)\sin(\theta_2-\theta_1+\theta_4-\theta_3)]2r_l\dot{\psi}^2\cos(\psi)$

$+ [(m_b+4m_1+4m_2)L^2 + (m_b+m_1+m_2)\, l_1^2 + (m_b+2m_1+m_2)\, 4r_l^2\cos^2(\psi) + (m_1+m_2)\, l_1^2 + m_2\, 4r_l^2\cos^2(\psi) + 2(m_b+2m_1+2m_2)Ll_1\sin(\theta_1) + 2(m_b+2m_1+2m_2)L2r_l\cos(\psi)\sin(\theta_1-\theta_2) + 4(m_b+m_1+m_2)\, l_1r_l\cos(\psi)\cos(\theta_2) - 4(m_1+m_2)\, Ll_1\sin(\theta_3) - 2(m_1+m_2)\, l_1^2\cos(\theta_1+\theta_3) - 4(m_1+m_2)\, l_1\, r_l\cos(\psi)\cos(\theta_1-\theta_2+\theta_3) - 4\, m_2\, Ll_0\sin(\theta_4-\theta_3) - 2\, m_2\, l_0\, l_1\cos(\theta_1+\theta_3-\theta_4) - 4\, m_2\, l_0\, r_l\cos(\psi)\cos(\theta_2-\theta_1+\theta_4-\theta_3) + 2\, m_2\, l_0\, l_1\cos(\theta_4) + m_b\, r_b^2]\ddot{\theta}$

$+ [-\, (m_b+m_1+m_2)\, l_1^2 - (m_b+2m_1+m_2)\, 4r_l^2\cos^2(\psi) - (m_b+2m_1+2m_2)L\, l_1\, \sin(\theta_1) - 2(m_b+2m_1+2m_2)\, L\, r_l\cos(\psi)\, \sin(\theta_1-\theta_2) - 4(m_b+m_1+m_2)\, l_1\, r_l\cos(\psi)\cos(\theta_2)+(m_1+m_2)\, l_1^2\cos(\theta_1+\theta_3) + 2(m_1+m_2)\, l_1\, r_l\cos(\psi)\cos(\theta_1-\theta_2+\theta_3) + m_2\, l_0\, l_1\cos(\theta_1+\theta_3-\theta_4) + 2m_2\, l_0\, r_l\cos(\psi)\cos(\theta_2-\theta_1+\theta_4-\theta_3)]\ddot{\theta}_1$

$+[(m_b+2m_1+m_2)4r_l^2\cos^2(\psi)+(m_b+2m_1+2m_2)Ll_2\sin(\theta_1-\theta_2)+2(m_b+m_1+m_2)l_1r_l\cos(\psi)\cos(\theta_2) - 2(m_1+m_2)\, l_1\, r_l\cos(\psi)\cos(\theta_1-\theta_2+\theta_3) - 2m_2\, l_0\, r_l\cos(\psi)\cos(\theta_2-\theta_1+\theta_4-\theta_3)]\ddot{\theta}_2$

$+ 2\quad (m_b+2m_1+m_2)2r_l\dot{\psi}\sin(\psi)(\dot{\theta}-\dot{\theta}_1+\dot{\theta}_2)+(m_b+2m_1+2m_2)Ll_1\dot{\theta}_1(2\dot{\theta}-\dot{\theta}_1)\quad \cos(\theta_1)\quad + (m_b+2m_1+2m_2)L[-2r_l\dot{\psi}\sin(\psi)(2\dot{\theta}-\dot{\theta}_1+\dot{\theta}_2)\sin(\theta_1-\theta_2)+(\dot{\theta}_1-\dot{\theta}_2)(2\dot{\theta}-\dot{\theta}_1+\dot{\theta}_2)\cos(\theta_1-\theta_2)+ 2r_l\dot{\psi}\sin(\psi)(\dot{\theta}_1-\dot{\theta}_2)\sin(\theta_1-\theta_2)] +(m_b+m_1+m_2)\, l_1\, [-2r_l\cos(\psi)\, \dot{\theta}_2(2\dot{\theta}-2\dot{\theta}_1+\dot{\theta}_2)\sin(\theta_2) -2r_l\dot{\psi}\sin(\psi)\, (2\dot{\theta}-2\dot{\theta}_1+\dot{\theta}_2)\cos(\theta_2) -2r_l\dot{\psi}\sin(\psi)\, \dot{\theta}_2\cos(\theta_2)] + (m_1+m_2)\, l_1^2\, \dot{\theta}_1\, (2\dot{\theta}-\dot{\theta}_1)\sin(\theta_1+\theta_3) + (m_1+m_2)\, l_1\, [2r_l\dot{\psi}\sin(\psi)\, (2\dot{\theta}-\dot{\theta}_1+\dot{\theta}_2)\cos(\theta_1-\theta_2+\theta_3) +2r_l\cos(\psi)\, (2\dot{\theta}-\dot{\theta}_1+\dot{\theta}_2)(\dot{\theta}_1-\dot{\theta}_2)\sin(\theta_1-\theta_2+\theta_3) -2r_l\dot{\psi}\sin(\psi)\, (\dot{\theta}_1-\dot{\theta}_2)\cos(\theta_1-\theta_2+\theta_3)] + m_2\, l_0\, l_1\, \dot{\theta}_1(2\dot{\theta}-\dot{\theta}_1)\, \sin(\theta_1+\theta_3-\theta_4) + m_2l_0[2r_l\dot{\psi}\sin(\psi)\, (2\dot{\theta}-\dot{\theta}_1+\dot{\theta}_2)\cos(\theta_2-\theta_1+\theta_4-\theta_3) + 2r_l\cos(\psi)\, (2\dot{\theta}-\dot{\theta}_1+\dot{\theta}_2)\, \sin(\theta_2-\theta_1+\theta_4-\theta_3) -2r_l\dot{\psi}\sin(\psi)\, (\dot{\theta}_1-\dot{\theta}_2)\sin(\theta_2-\theta_1+\theta_4-\theta_3)]$

$+g[(m_b+2m_1+2m_2)L\cos(\theta+\theta_p)+(m_b+m_1+m_2)l_1\sin(\theta_1-(\theta+\theta_p))-(m_b+2m_1+m_2)2r_l\cos(\psi)\, \sin(\theta_2-\theta_1+\theta+\theta_p) + (m_1+m_2)\, l_1\, \sin(\theta+\theta_p+\theta_3)-m_2l_0\sin(\theta_4-(\theta+\theta_p+\theta_3))]$

$$= 0$$

Equation of motion for generalized coordinate θ_1

By direct substitution of equation (2.28) in the below equation, the equation of motion for generalised coordinate θ_1 can be calculated

$$\frac{d}{dt}\left(\frac{DL}{D\dot{\theta}_1}\right) - \frac{DL}{D\theta_1} + \frac{DB}{D\dot{\theta}_1} = \tau_1$$

The equation of motion for generalised Coordinate θ_1 becomes,

$[l_1(m_b + m_1 + m_2)\sin(\theta_2)]\, 2r_l\dot{\psi}^2\cos(\psi) + [-l_1{}^2(m_b + m_1 + m_2) - 4r_l^2\cos^2(\psi)(m_b + 2m_1 + m_2)$

$+ -Ll_1(m_b + 2m_1 + 2m_2)\sin(\theta_1) - 4l_1r_l\cos(\psi)(m_b + m_1 + m_2)\cos(\theta_2) + (m_1 +$

$m_2)l_1{}^2\cos(\theta_1 + \theta_3)$ $+$

$2(m_1 + m_2)l_1r_l\cos(\psi)\cos(\theta_1 - \theta_2 + \theta_3) + 2m_2l_1r_l\cos(\psi)\cos(\theta_1 + \theta_3 - \theta_4)$ $+$

$2m_2r_l\cos(\psi)l_0\cos(\theta_2 - \theta_1 + \theta_4 - \theta_3) - 2Lr_l\cos(\psi)(m_b + 2m_1 + 2m_2)\sin(\theta_1 - \theta_2)]\,\ddot{\theta}$

$+\ \ [l_1{}^2(m_b + m_1 + m_2) + m_1r_1{}^2 + 4r_l^2\cos^2(\psi)(m_b + 2m_1 + m_2) + 4l_1r_l\cos(\psi)(m_b + m_1 +$

$m_2)\cos(\theta_2)]\,\ddot{\theta}_1$

$+ [-4r_l^2\cos^2(\psi)(m_b + 2m_1 + m_2) - 2l_1r_l\cos(\psi)(m_b + m_1 + m_2)\cos(\theta_2)]\,\ddot{\theta}_2$

$+ 4(m_b + 2m_1 + 2m_2)l_2r_l\dot{\psi}\sin(\psi)(\dot{\theta} + \dot{\theta}_2 - \dot{\theta}_1) + (m_b + 2m_1 + 2m_2)[-Ll_1\dot{\theta}^2\cos(\theta_1) -$

$2Lr_l\cos(\psi)\dot{\theta}^2\cos(\theta_1 - \theta_2)]$ $+$

$(m_b + m_1 + m_2)l_1[2r_l\dot{\psi}\sin(\psi)(2\dot{\theta}_2 - 2\dot{\theta}_1 + 2\dot{\theta})\cos(\theta_2) + 2r_l\cos(\psi)\dot{\theta}_2(\dot{\theta}_2 - 2\dot{\theta}_1 +$

$2\dot{\theta})\sin(\theta_2)]$

$+ (m_1 + m_2)[-l_1{}^2\dot{\theta}^2\sin(\theta_1 + \theta_3) - 2l_1r_l\cos(\psi)\dot{\theta}^2\sin(\theta_1 - \theta_2 + \theta_3)]$

$+ m_2[-2l_1r_l\cos(\psi)\dot{\theta}^2\sin(\theta_1 + \theta_3 - \theta_4) + 2r_l\cos(\psi)r_l\cos(\psi)\dot{\theta}^2\sin(\theta_2 - \theta_1 + \theta_4 - \theta_3)]$

$+ g[-(m_b + m_1 + m_2)l_1\sin(\theta_1 - (\theta + \theta_p)) + 2(m_b + 2m_1 + m_2)r_l\cos(\psi)\sin(\theta_2 - \theta_1 +$

$\theta + \theta_p)]$

$= \tau_1$

Equation of motion for generalized coordinate θ_2

By direct substitution of equation (2.28) in the below equation, the equation of motion for generalised coordinate θ_2 can be calculated

$$\frac{d}{dt}\left(\frac{DL}{D\dot{\theta}_2}\right) - \frac{DL}{D\theta_2} + \frac{DB}{D\dot{\theta}_2} = \tau_2$$

The equation of motion for generalised Coordinate θ_2 becomes,

$[4(m_b+2m_1 + m_2)r_l^2\cos^2(\psi) + 2(m_b+2m_1 + 2m_2)Lr_l\cos(\psi)\sin(\theta_1 - \theta_2)+2(m_b+m_1 + m_2)l_1r_l\cos(\psi)\cos(\theta_2)$

$-2(m_1 + m_2)l_1r_l\cos(\psi)\cos(\theta_1 - \theta_2 + \theta_3) - 2m_2r_l\cos(\psi)\cos(\theta_2 - \theta_1 + \theta_4-\theta_3)]\ddot{\theta}$

$[-4r_l^2\cos^2(\psi)(m_b+2m_1 + m_2) - 2l_1r_l\cos(\psi)(m_b+m_1 + m_2)\cos(\theta_2)]\ddot{\theta}_1 \qquad +$

$[4r_l^2\cos^2(\psi)(m_b+2m_1 + m_2) + m_2r_2{}^2]\ddot{\theta}_2+4(m_b+2m_1 + 2m_2)Lr_l^2\cos^2(\psi)\dot{\theta}^2\cos(\theta_1 - \theta_2)$

$+ 2(m_b+m_1 + m_2)l_1r_l\cos(\psi)(\dot{\theta} - \dot{\theta}_1)^2\sin(\theta_2)$

$+(m_1 + m_2)[2l_1r_l\cos(\psi)\dot{\theta}^2\sin(\theta_1 - \theta_2 + \theta_4)]+ \qquad 2m_2r_l\cos(\psi)[-2r_l\cos(\psi)\dot{\theta}^2\sin(\theta_2 - \theta_1 + \theta_4-\theta_3)]$

$-g[2(m_b+2m_1 + m_2)r_l\cos(\psi)\sin(\theta_2 - \theta_1 + \theta + \theta_p)] -$

$4(m_b+2m_1 + m_2)r_l^2\dot{\psi}\sin(2\psi)(\dot{\theta} + \dot{\theta}_2 - \dot{\theta}_1)$

$=\tau_2$

2.3 Flight after back stance phase

Cartesian coordinates

$$P = \begin{bmatrix} X_{lo,b} + \dot{X}_{lo,b}t \\ -\frac{1}{2}gt^2 + \dot{Y}_{lo,b}t + Y_{lo,b} \end{bmatrix}$$

Velocities

$$\dot{P} = \begin{bmatrix} \dot{X}_{lo,b} \\ -gt + \dot{Y}_{lo,b} \end{bmatrix}$$

Body pitch

$$\theta = \theta_{lo,b} + \dot{\theta}_{lo,b}t$$
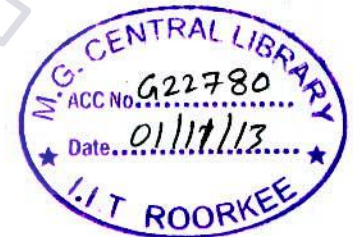
Body pitch speed

$$\dot{\theta} = \dot{\theta}_{lo,b}$$

Leg angle

$$\begin{cases} \theta_1 = \theta_{lo,1b} + \dot{\theta}_{1b}t \\ \theta_2 = \theta_{lo,2b} + \dot{\theta}_{2b}t \\ \theta_3 = \theta_{lo,3b} + \dot{\theta}_{3b}t \\ \theta_4 = \theta_{lo,4b} + \dot{\theta}_{4b}t \end{cases}$$

Leg angle speed

$$\begin{cases} \theta_1 = \dot{\theta}_{1b} \\ \theta_2 = \dot{\theta}_{2b} \\ \theta_3 = \dot{\theta}_{3b} \\ \theta_4 = \dot{\theta}_{4b} \end{cases}$$

19

2.4 Front Stance

The Kinetic and Potential energies of the various links in the Front Stance phase of the robot were calculated for the below geometry. Further, the Lagrangian Function (L) was calculated following the procedure similar to the Back Stance phase.
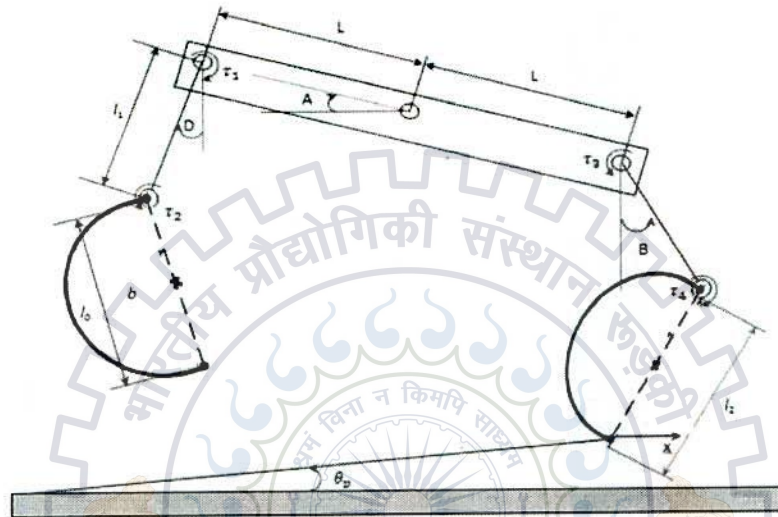

Figure 2.2: Front Stance Configuration

Where,

$$A = \theta - \theta_p$$

$$B = \theta_3 - \theta + \theta_p$$

$$C = \theta_4 - \theta_3 + \theta - \theta_p$$

$$D = \theta - \theta_p + \theta_1$$

$$E = \theta_2 - \theta_1 - \theta + \theta_p$$

After the Lagrangian Function (L) was found the Equations of motion for the different generalised co-ordinates are to be found.

19

Equation of motion for generalized coordinate ψ

By direct substitution of equation (2.88) in the below equation, the equation of motion for generalised coordinate l_2 can be calculated

$$\frac{d}{dt}\left(\frac{DL}{D\dot{\psi}}\right) - \frac{DL}{D\psi} + \frac{DB}{D\dot{\psi}} = F$$

The equation of motion for generalised Coordinate ψ becomes,

$-2(m_b+2m_1+2m_2)r_l\dot{\psi}^2\cos(\psi) + \big[L(m_b+2m_1+2m_2)\cos(\theta_3-\theta_4) + l_1(m_b+m_1+m_2)\sin(\theta_4) - l_1(m_1+m_2)\sin(\theta_4-\theta_3-\theta_1) + 2m_2r_l\cos(\psi)\sin(\theta_4-\theta_3-\theta_2+\theta_1+2(\theta-\theta_p))\big]\ddot{\theta} - [l_1(m_b+m_1+m_2)\sin(\theta_4)]\ddot{\theta}_1 - [(m_b+2m_1+m_2)]l_2\left(\dot{\theta}+\dot{\theta}_4-\dot{\theta}_3\right)^2 + k\cos(constant(\psi+\psi_0))(2r_l\cos(\psi)-l_0)$

$+ [L(m_b+2m_1+2m_2)]\dot{\theta}^2\sin(\theta_3-\theta_4) - [l_1(m_b+m_1+m_2)]\left(\dot{\theta}-\dot{\theta}_3\right)^2\cos(\theta_4) + [l_1(m_1+m_2)]\dot{\theta}^2\cos(\theta_4-\theta_3-\theta_1) + m_2l_0\dot{\theta}\big[(2\dot{\theta}+\dot{\theta}_4-\dot{\theta}_3)\cos(\theta_4-\theta_3-\theta_2+\theta_1+2(\theta-\theta_p)) - (\dot{\theta}+\dot{\theta}_4-\dot{\theta}_3)\cos(\theta_4-\theta_3+\theta_2-\theta_1)\big] + [g(m_b+2m_1+m_2)]\cos(\theta_4-\theta_3+\theta-\theta_p) = F_i\cos(\theta_4-\theta_3+\theta-\theta_p) + \mu F_i\cos(\theta_4-\theta_3+\theta-\theta_p)$

Equation of motion for generalized coordinate θ

By direct substitution of equation (2.88) in the below equation, the equation of motion for generalised coordinate θ can be calculated

$$\frac{d}{dt}\left(\frac{DL}{D\dot{\theta}}\right) - \frac{DL}{D\theta} + \frac{DB}{D\dot{\theta}} = 0$$

The equation of motion for generalised Coordinate θ becomes,

$[(m_b+2m_1+2m_2)L\cos(\theta_3-\theta_4)+(m_b+m_1+m_2)l_1\sin(\theta_4)-(m_1+m_2)l_1\sin(\theta_4-\theta_3-\theta_1)$
$-2m_2l_0\sin(\theta_4-\theta_3-\theta_2+\theta_1+2(\theta-\theta_p))]r_l\ddot{\psi}^2\cos(\psi)l_2+[(m_b+4m_1+4m_2)L^2+(m_b+2m_1+2m_2)l_1^2+m_br_b^2+m_2l_0^2+8r_l\cos(\psi)(m_b+2m_1+m_2)\ r_l^2\cos^2(\psi)+2(m_b+2m_1+m_2)Ll_1\sin(\theta_3)+2(m_b+2m_1+2m_2)2Lr_l\cos(\psi)\sin(\theta_3-\theta_4)+4(m_b+m_1+m_2)\ l_1\ r_l\cos(\psi)\cos(\theta_4)+4(m_1+m_2)\ Ll_1\sin(\theta_1)-2(m_1+m_2)\ l_1^2\cos(\theta_1+\theta_3)-4(m_1+m_2)\ l_1\ r_l\cos(\psi)\cos(\theta_4-\theta_3-\theta_1)-4\ m_2\ Ll_0\ \sin(\theta_1-\theta_2+2(\theta-\theta_p))+2\ m_2\ l_0\ l_1\cos(\theta_3+\theta_1-\theta_2)+4\ m_2\ l_0\ r_l\cos(\psi)\ \cos(\theta_4-\theta_3+\theta_2-\theta_1)-2\ m_2\ l_0\ l_1\cos(\theta_2+2(\theta_1+\theta-\theta_p))]\ \ddot{\theta}$

$+ \qquad\qquad [-(m_b+m_1+m_2)l_1{}^2-4(m_b+2m_1+m_2)r_l^2\cos^2(\psi)-(m_b+2m_1+2m_2)Ll_1\sin(\theta_3)-$

$2(m_b+2m_1+2m_2)Lr_l\cos(\psi)\sin(\theta_3-\theta_4)-4(m_b+m_1+m_2)l_1r_l\cos(\psi)\cos(\theta_4)+(m_1+m_2)$

$l_1{}^2\cos(\theta_1+\theta_3) + 2(m_1+m_2)\, l_1\, r_l\cos(\psi)\cos(\theta_4-\theta_3-\theta_1) + m_2\, l_0\, l_1\, \cos(\theta_3+\theta_1-\theta_2) - 2m_2\, l_0$

$r_l\cos(\psi)\,\cos(\theta_4-\theta_3+\theta_2-\theta_1)\,]\,\ddot\theta_1$

$+4\,[(m_b+2m_1+m_2)\, r_l^2\cos^2(\psi) + 2(m_b+2m_1+2m_2)\, L\, r_l\cos(\psi)\sin(\theta_3-\theta_4) + (m_b+m_1+m_2)\, l_1$

$l_2\cos(\theta_4) - 2(m_1+m_2)l_1r_l\cos(\psi)\cos(\theta_4-\theta_3-\theta_1)+2m_2l_0r_l\cos(\psi)\,\cos(\theta_2-\theta_1+\theta_4-\theta_3)]\ddot\theta_2$

$- 8(m_b+2m_1+m_2)\, r_l\cos(\psi)\, r_l\dot\psi\sin(\psi)(\dot\theta-\dot\theta_3+\dot\theta_4) - (m_b+2m_1+2m_2)L\, l_1\dot\theta_1(\dot\theta_1-2\dot\theta)\,\cos(\theta_3)$

$+(m_b+2m_1+2m_2)L[-2r_l\dot\psi\sin(\psi)(2\dot\theta-\dot\theta_3+\dot\theta_4)\sin(\theta_3-\theta_4)+2r_l\cos(\psi)(\dot\theta_3-\dot\theta_4)(2\dot\theta-$

$\dot\theta_3+\dot\theta_4)\cos(\theta_3-\theta_4)+2r_l\dot\psi\sin(\psi)\quad(\dot\theta_3-\dot\theta_4)\sin(\theta_3-\theta_4)]\quad+(m_b+m_1+m_2)l_1[2r_l\cos(\psi)\quad\dot\theta_4$

$(2\dot\theta_3-2\dot\theta-\dot\theta_4)\sin(\theta_4)+2r_1\dot\psi\sin(\psi)(2\dot\theta_3-2\dot\theta-\dot\theta_4)\cos(\theta_4)]+(m_1+m_2)l_1[-l_1{}^2\dot\theta_3(\dot\theta_3-$

$2\dot\theta)\sin(\theta_1+\theta_3)\ +4r_1\dot\psi\sin(\psi)\ (\dot\theta-\dot\theta_3+\dot\theta_4)\cos(\theta_4-\theta_3-\theta_1)\ +2r_l\cos(\psi)\ (2\dot\theta-\dot\theta_3+\dot\theta_4)$

$(\dot\theta_4-\dot\theta_3)\,\sin(\theta_4-\theta_3-\theta_1)]$

$+m_2l_0[-8L\dot\theta^2\cos(\theta_1-\theta_2+2(\theta-\theta_p))+l_1(\dot\theta_3-2\dot\theta)\,\dot\theta_3\sin(\theta_1+\theta_3-\theta_2)-2r_1\dot\psi\sin(\psi)(\dot\theta_4-$

$\dot\theta_3+2\dot\theta)\cos(\theta_4-\theta_3-\theta_2+\theta_1+2(\theta-\theta_p))-2r_1\dot\psi\sin(\psi)(\dot\theta_4-\dot\theta_3+2\dot\theta)\cos(\theta_4-\theta_3-\theta_2+$

$\theta_1)+ l_2(\dot\theta_4-\dot\theta_3+2\dot\theta)(\dot\theta_4-\dot\theta_3)\,\sin(\theta_2-\theta_1+\theta_4-\theta_3)+2l_1l_0\,\dot\theta^2\,\sin(\theta_2+2(\theta_1+\theta-\theta_p))+$

$4Ll_0\dot\theta^2\,\cos(\theta_1-\theta_2+2(\theta-\theta_p))-4r_1\dot\psi\sin(\psi)\dot\theta\,\cos(\theta_4-\theta_3+\theta_1-\theta_2+2(\theta-\theta_p))$

$+ \; g[(m_b+2m_1+2m_2)L\;\cos(\theta-\theta_p)\;+\;(m_b+m_1+m_2)\;l_1\;\sin(\theta_3-(\theta-\theta_p))-\;(m_b+2m_1+m_2)$

$2r_l\cos(\psi)\sin(\theta_4-\theta_3+\theta-\theta_p)\;+\;(m_1+m_2)\;l_1\;\sin(\theta-\theta_p+\theta_1)-\;m_2\;l_0\;\cos(\theta_2-(\theta-$

$\theta_p+\theta_1))]$

$= 0$

Equation of motion for generalized coordinate θ_3

By direct substitution of equation (2.88) in the below equation, the equation of motion for generalised coordinate θ_3 can be calculated

$$\frac{d}{dt}\left(\frac{DL}{D\dot\theta_3}\right) - \frac{DL}{D\theta_3} + \frac{DB}{D\dot\theta_3} = \tau_3$$

The equation of motion for generalised Coordinate θ_3 becomes,

$[+2l_1(m_b+m_1+m_2)\sin(\theta_2)]\dot\psi^2\cos(\psi)$ $\qquad\qquad\qquad +$

$[-l_1{}^2(m_b+m_1+m_2) - 4r_l^2\cos^2(\psi)(m_b+2m_1+m_2)$

$-Ll_1(m_b+2m_1+2m_2)\sin(\theta_3) + 4l_1r_l\cos(\psi)(m_b+m_1+m_2)\cos(\theta_4)+(m_1+m_2)$

$l_1{}^2\cos(\theta_3+\theta_1)\ \ +2(m_1+m_2)l_1r_l\cos(\psi)\cos(\theta_4-\theta_3-\theta_1)-m_2l_1l_0\cos(\theta_3+\theta_3-\theta_4)$

$- 2mr_l\cos(\psi)l_0\cos(\theta_4-\theta_3+\theta_2-\theta_1) - 2Lr_l\cos(\psi)(m_b+2m_1+2m_2)\sin(\theta_3-\theta_4)\,]\,\ddot\theta$

22

$$+[l_1{}^2(m_b+m_1+m_2)+m_1r_1{}^2+4r_l^2\cos^2(\psi)(m_b+2m_1+m_2)+2l_1r_l\cos(\psi)(m_b+m_1+m_2)]\ddot\theta_3$$

$$+[-4r_l^2\cos^2(\psi)(m_b+2m_1+m_2)-2r_l\cos(\psi)l_1(m_b+m_1+m_2)]\ddot\theta_4 + [4(m_b+2m_1+m_2)l_2r_l\dot\psi\sin(\psi)(\dot\theta+\dot\theta_4-\dot\theta_3)+$$

$$(m_b+2m_1+2m_2)[-Ll_1\dot\theta^2\cos(\theta_3)-2Lr_l\cos(\psi)\dot\theta^2\cos(\theta_3-\theta_4)]$$

$$+ (m_b+m_1+m_2)l_1[2r_l\dot\psi\sin(\psi)(2\dot\theta_4-\dot\theta_3+\dot\theta)\cos(\theta_4)+2r_l\cos(\psi)\dot\theta_4(\dot\theta_4-\dot\theta_3+\dot\theta)\sin(\theta_4)]$$

$$+(m_1+m_2)[-l_1{}^2\dot\theta^2\sin(\theta_3+\theta_1)+2l_1r_l\cos(\psi)\dot\theta^2\sin(\theta_4-\theta_3-\theta_1)]$$

$$+m_2[l_1l_0\dot\theta^2\sin(\theta_3+\theta_1-\theta_2)-2l_0r_l\dot\psi\sin(\psi)\dot\theta\cos(\theta_4-\theta_3-\theta_2+\theta_1+2(\theta-\theta_p))-$$

$$2l_0r_l\cos(\psi)\dot\theta^2\sin(\theta_4-\theta_3+\theta_2-\theta_1)]+g[-(m_b+m_1+m_2)l_1\sin(\theta_3-\theta+\theta_p)+$$

$$2(m_b+2m_1+m_2)r_l\cos(\psi)\sin(\theta_4-\theta_3+\theta-\theta_p)] \qquad = \qquad \tau_3$$

Equation of motion for generalized coordinate θ_4

By direct substitution of equation (2.88) in the below equation, the equation of motion for generalised coordinate θ_4 can be calculated,

$$\frac{d}{dt}\left(\frac{DL}{D\dot\theta_4}\right)-\frac{DL}{D\theta_4}+\frac{DB}{D\dot\theta_4}=\tau_4$$

The equation of motion for generalised Coordinate θ_4 becomes,

$$[4(m_b+2m_1+m_2)r_l^2\cos^2(\psi)+2(m_b+2m_1+m_2)Lr_l\cos(\psi)\sin(\theta_3-\theta_4)+2(m_b+m_1+m_2)l_1r_l\cos(\psi)\cos(\theta_4)$$

$$-2(m_1+m_2)l_1r_l\cos(\psi)\cos(\theta_4-\theta_3-\theta_1)+2m_2l_0r_l\cos(\psi)\cos(\theta_4-\theta_3+\theta_2-\theta_1)]\ddot\theta$$

$$[-4r_l^2\cos^2(\psi)(m_b+2m_1+m_2)-2l_1r_l\cos(\psi)(m_b+m_1+m_2)\cos(\theta_4)]\ddot\theta_1$$

$$+[4r_l^2\cos^2(\psi)(m_b+2m_1+m_2)]\ddot\theta_4$$

$$-4(m_b+2m_1+m_2)l_2r_l\dot\psi\sin(\psi)(\dot\theta+\dot\theta_4-\dot\theta_3)-2(m_b+2m_1+m_2)Lr_l\dot\psi\sin(\psi)\dot\theta\sin(\theta_3-\theta_4)+2(m_b+2m_1+2m_2)Lr_l\cos(\psi)\dot\theta\cos(\theta_3-\theta_4)+2(m_b+m_1+m_2)l_1r_l\cos(\psi)(\dot\theta_3-\dot\theta)^2\sin(\theta_4)+$$

$$(m_b+2m_1+2m_2)L(2r_l\cos(\psi)\dot\theta(\dot\theta+\dot\theta_4-\dot\theta_3)\cos(\theta_3-\theta_4)+2r_l\dot\psi\sin(\psi)\dot\theta\sin(\theta_3-\theta_4))$$

$$+(m_1+m_2)[-2l_1r_l\cos(\psi)\dot\theta^2\sin(\theta_4-\theta_3-\theta_1)] + m_2l_0[-2r_l\dot\psi\sin(\psi)\dot\theta\cos(\theta_4-\theta_3+\theta_2-\theta_1)+2r_l\dot\psi\sin(\psi)\dot\theta\cos(\theta_4-\theta_3-\theta_2+\theta_1+2(\theta-\theta_p))+2r_l\cos(\psi)\dot\theta^2\sin(\theta_4-\theta_3+\theta_2-\theta_1)]-g[(m_b+2m_1+m_2)2r_l\cos(\psi)\sin(\theta_4-\theta_3+\theta-\theta_p)]$$

$$=\tau_4$$

23

2.4 Flight after front stance phase

Cartesian coordinates

$$P = \begin{bmatrix} X_{lo,f} + \dot{X}_{lo,f}t \\ -\frac{1}{2}gt^2 + \dot{Y}_{lo,f}t + Y_{lo,f} \end{bmatrix}$$

Velocities

$$\dot{P} = \begin{bmatrix} \dot{X}_{lo,f} \\ -gt + \dot{Y}_{lo,f} \end{bmatrix}$$

Body pitch

$$\theta = \theta_{lo,f} + \dot{\theta}_{lo,f}t$$

Body pitch speed

$$\dot{\theta} = \dot{\theta}_{lo,f}$$

Leg angle

$$\begin{cases} \theta_1 = \theta_{lo,1f} + \dot{\theta}_{1f}t \\ \theta_2 = \theta_{lo,2f} + \dot{\theta}_{2f}t \\ \theta_3 = \theta_{lo,3f} + \dot{\theta}_{3f}t \\ \theta_4 = \theta_{lo,4f} + \dot{\theta}_{4f}t \end{cases}$$

Leg angle speed

$$\begin{cases} \theta_1 = \dot{\theta}_{1f} \\ \theta_2 = \dot{\theta}_{2f} \\ \theta_3 = \dot{\theta}_{3f} \\ \theta_4 = \dot{\theta}_{4f} \end{cases}$$

CHAPTER 3   SIMULINK MODELS AND RESULTS

3.1 Simulink Model

Simulation of quadruped robot with flexible legs can be done by Matlab/Simulink package. It is graphical extension of MATLAB for modelling, simulating and analysing a variety of dynamical systems under Graphical user interface (GUI) environment. In Simulink, models of the systems are drawn on screen as block diagrams. It includes a comprehensive block library for creating standard components such as sinks, sources, connectors, linear and non linear components.

To make a model for any particular system, the components required for the model are selected from Library Browser and are then dragged and dropped in Simulink window. Any block library can be detailed by clicking on it and the desired block can be selected. It is integrated with MATLAB and data can be easily transferred between the programs. Different blocks are then connected as per the model requirement by arranging them and drawing connecting lines from the output terminal of the block to the input terminal of the other block.

The various steps taken to make a complete model are as follows:

1. Collecting blocks to create model
2. Modifying block parameters
3. Labelling blocks
4. Connecting blocks
5. Labelling the signal lines
6. Saving the model

Simulink Modeling for the various stances and the C-leg(Link) robot was done in order to obtain the various positions and velocities of the joints and the change in stiffness of the C-leg(Link).

3.1.1 Back Stance Model

The figure 3.1 below shows the Simulink Model for the Back Stance phase of the locomotion of the robot. Different subsystems for the various generalized co-ordinates are created and the whole system is modeled.
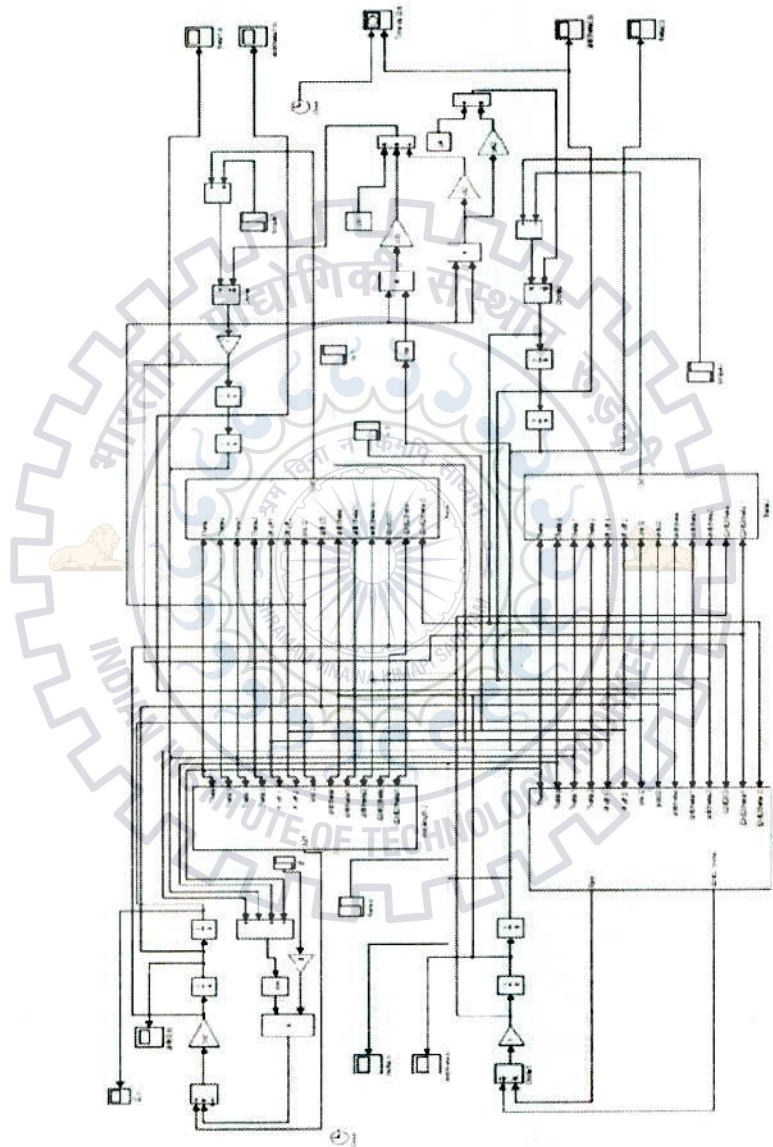

Figure 3.1: Simulink Model for Back Stance Phase

The Simulink model for the inclusion of the Variable Compliant C-leg in the Back Stance is shown below. The Variable Stiffness function block and the C-leg Geometry function block are clearly visible in the model below (Fig. 3.2).
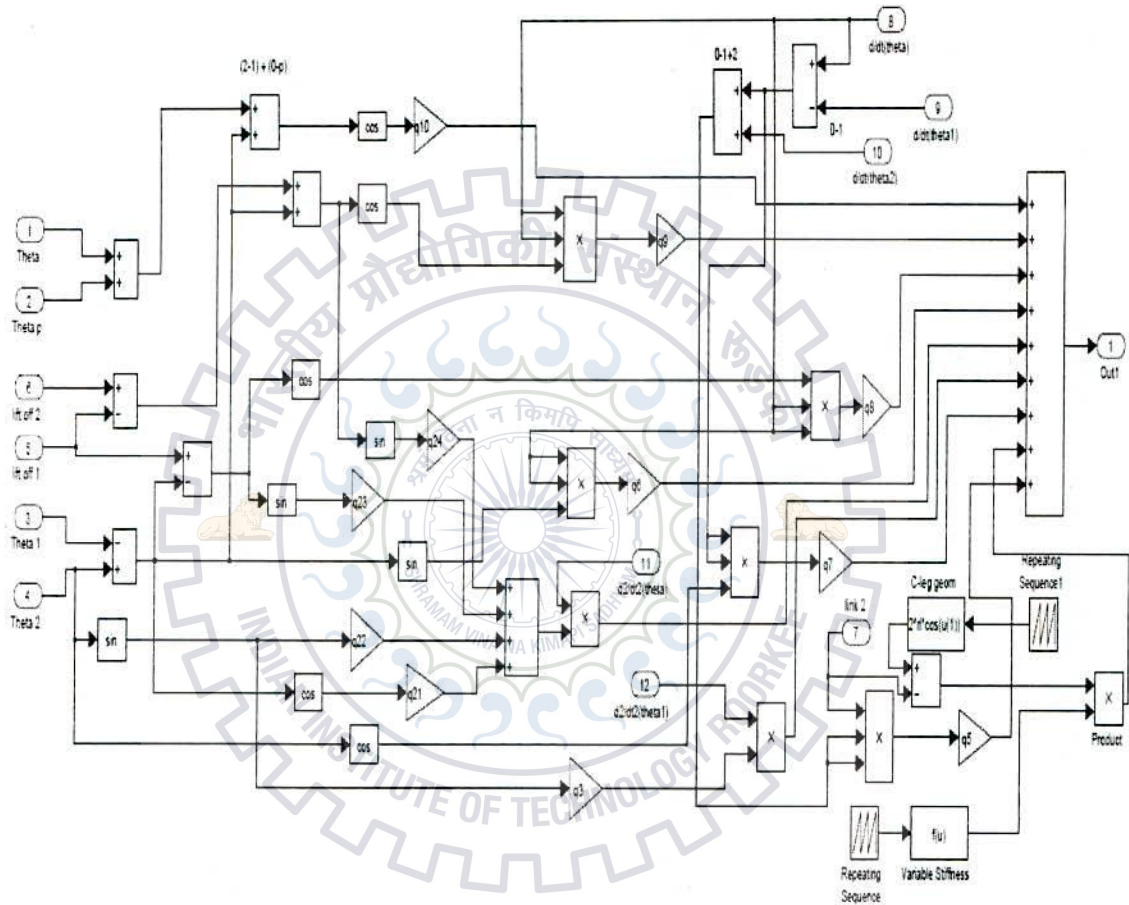
Figure 3.2: Simulink model for inclusion of Variable Compliant C-leg

3.1.2 Front Stance Model

This is the Simulink Model for the Front Stance phase of the locomotion of the robot. Different subsystems for the various generalized co-ordinates are created and the whole system is modeled.
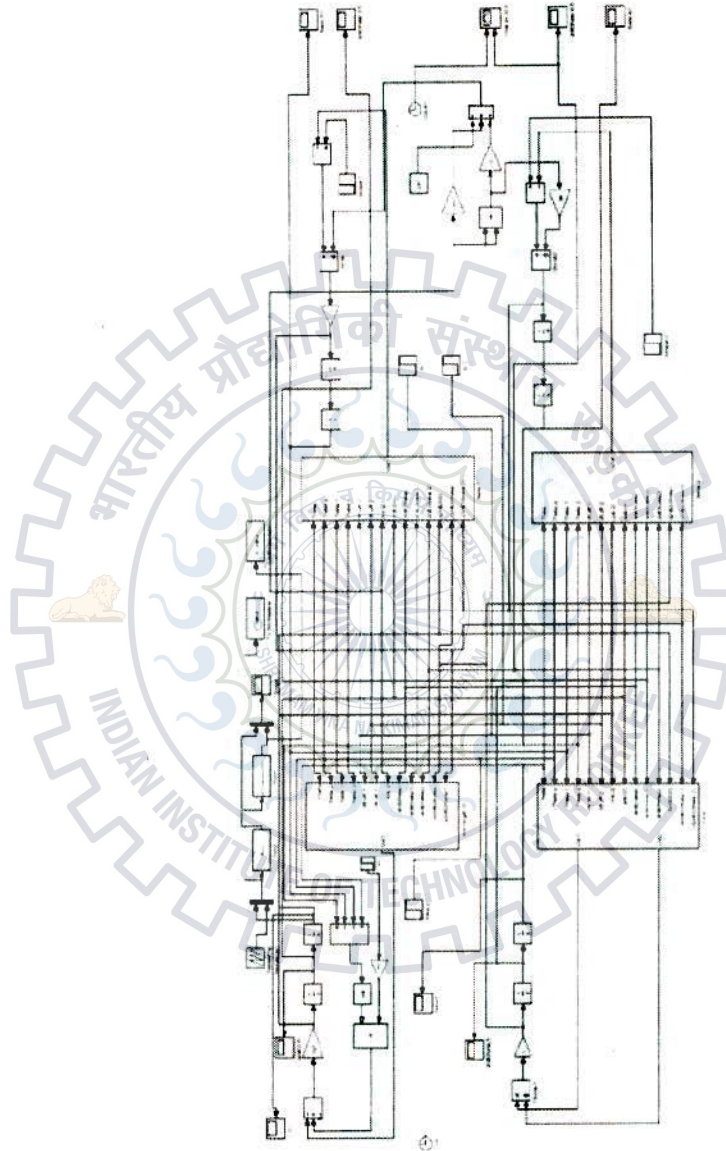

Figure 3.3: Simulink Model for the Front Stance phase

28

The Simulink model for the inclusion of the Variable Compliant C-leg in the Back Stance is shown below. The Variable Stiffness function block and the C-leg Geometry function block are clearly visible in the model below (Fig. 3.4).
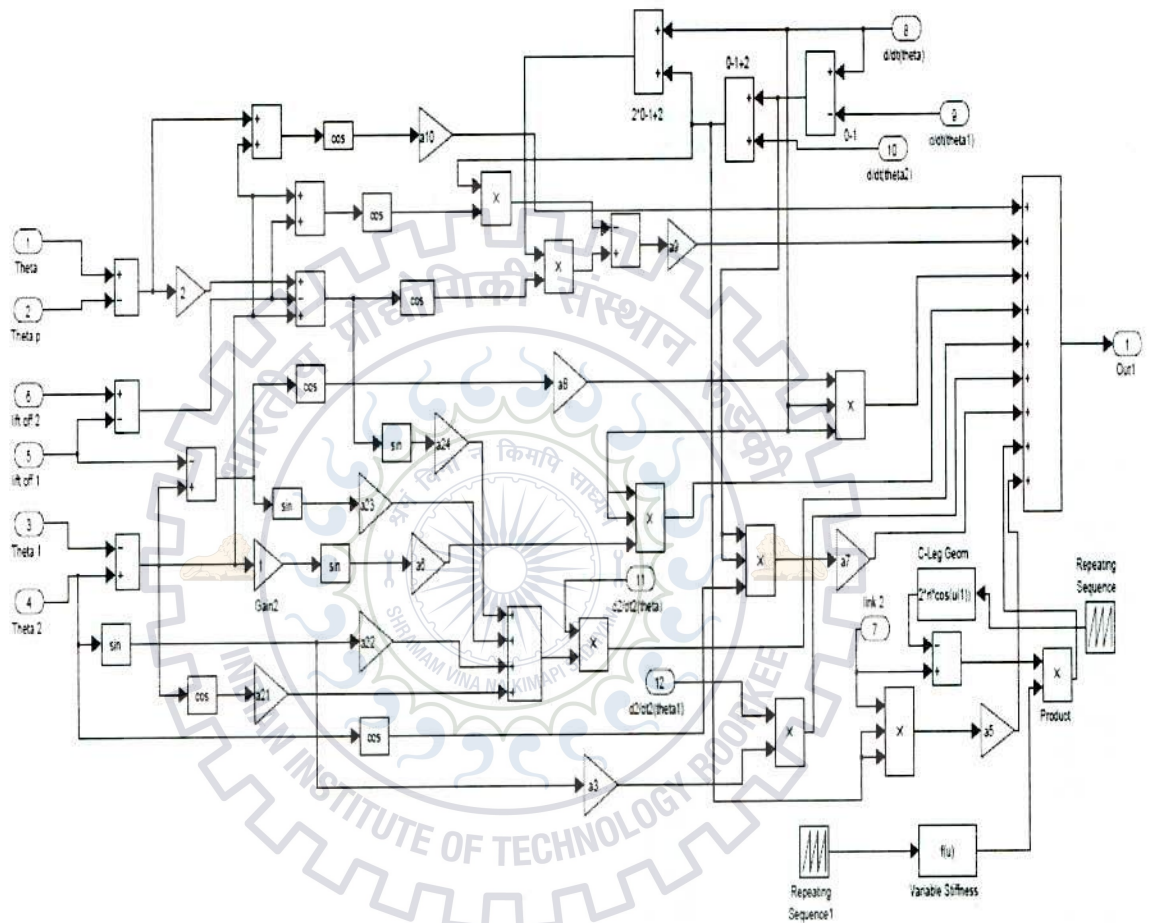

Figure 3.4: Simulink Model for inclusion of Variable Compliant C-leg in Back Stance

3.1.3 Back Flight and Front Flight Models

This is the Simulink Model for the Back Flight and Front Flight phases of the locomotion of the robot. The X and Y co-ordinates of all the joints during the cycle of the two different phases are found out in these models (Fig. 3.5 and 3.6).
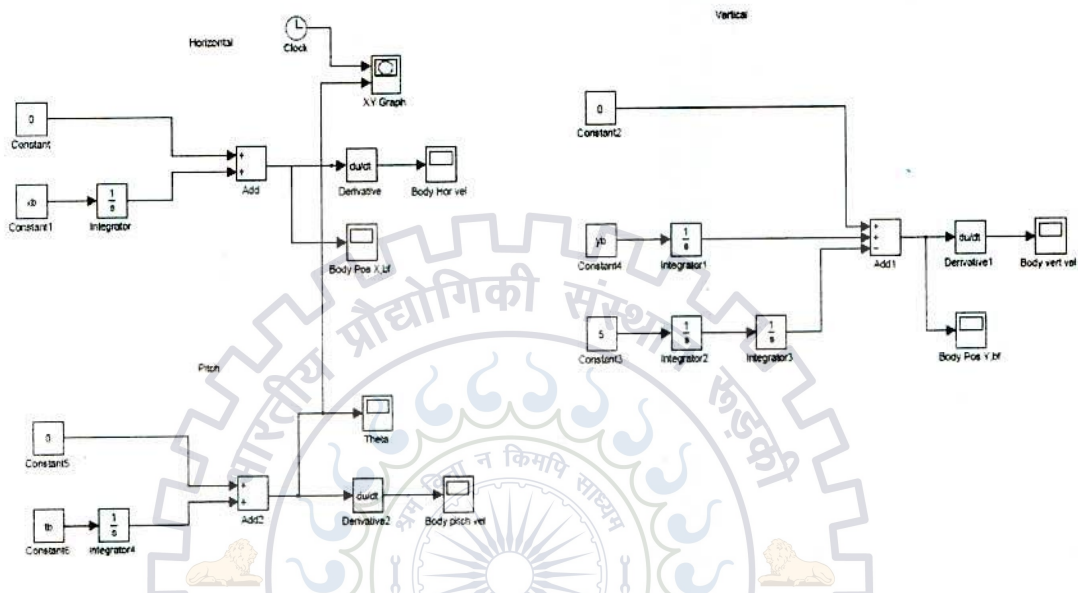
Back Flight Model

Figure 3.5: Simulink Model for the Back Flight Phase
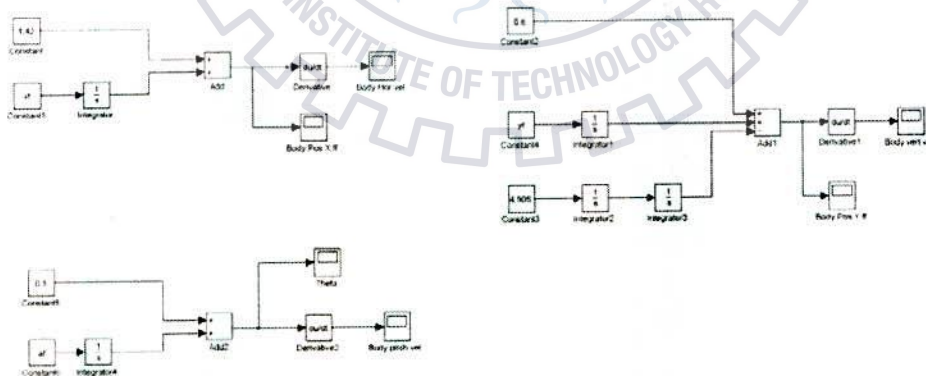
Front Flight Model

Figure 3.6: Simulink Model for the Front Flight Phase

3.1.4 The Simulink Model for the Overall Locomotion for 10 seconds

This is the base model where all the various subsystems, designed for different time period, are clubbed for the locomotion of the four legged robot in a sagittal plane for the period of 10 seconds.
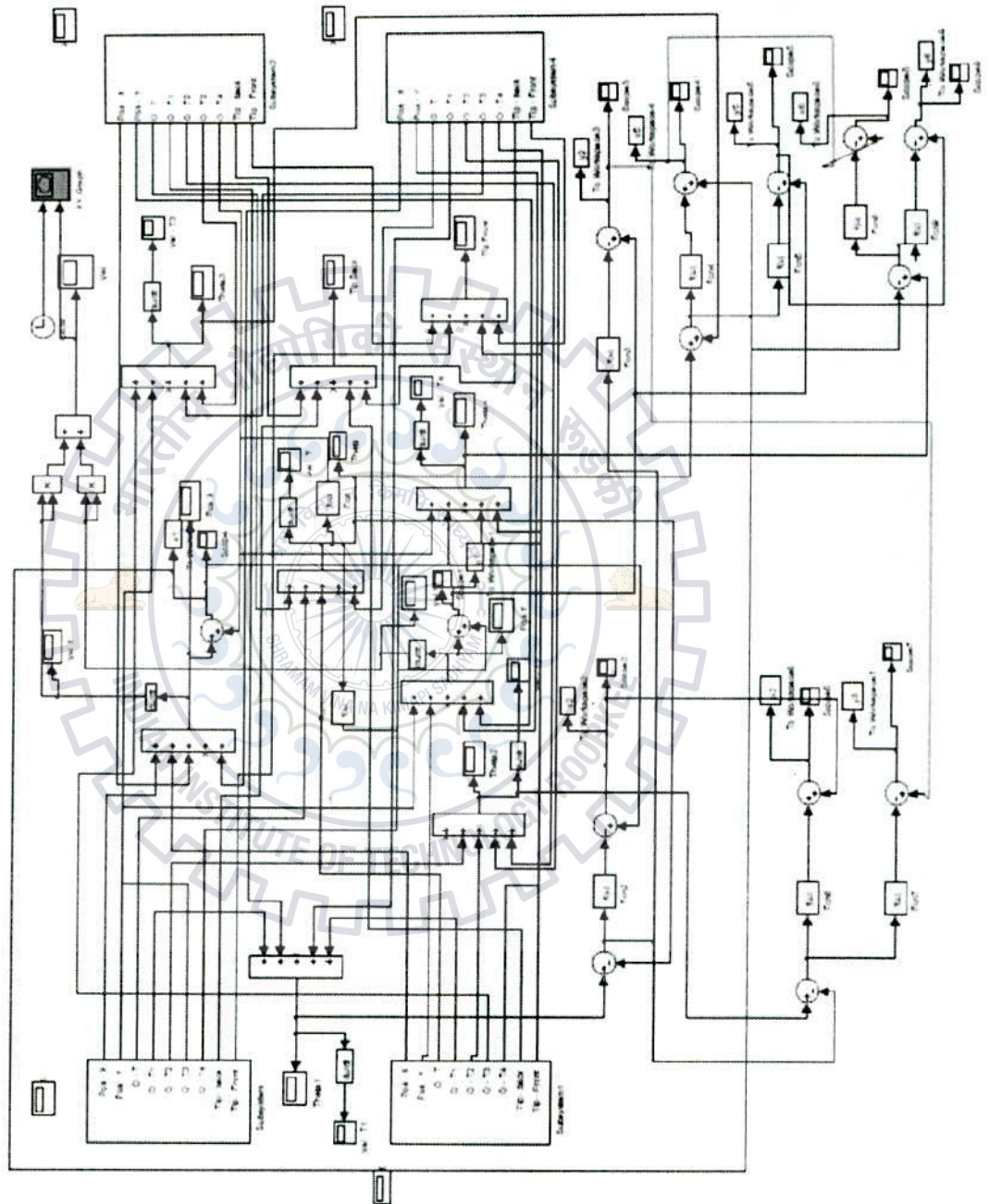

Figure 3.7: Simulink Base Model for the locomotion for 10 seconds

3.2 Initial Conditions and Model Parameters

Once the Simulink model is made, it is simulated for the set of initial conditions. While starting the simulation it is assumed that robot is in home position. So the set of initial conditions for the four legged robot is given in the table.

Table 1: Initial conditions of State variables

State Variables	θ	θ_1	θ_2	θ_3	θ_4	ψ/ψ_0
Initial Conditions	0 rad	0 rad	0 rad	0 rad	0 rad	-0.8722 rad

The model parameters used in the simulation are given in table 2.[10]

Table 2: Physical Parameters

Parameter	Symbol	Value
Body Mass	M	23 Kg
Leg Mass	m_1	0.85 Kg
Leg Mass	m_2	0.82 Kg
Body Inertia	I	1.091 Kg-m^2
Leg Inertia for link 1	I_1	0.020 Kg-m^2
Leg Inertia for link 2	I_2	0.019 Kg-m^2
Hip Length	$2L$	0.8 m
Leg Length link 1	l_1	0.325 m
Leg Length link 2	l_2	0.325 m
Friction factor	μ	0.35
Leg Spring Constant	K	3600 N/m
Constant	C	10
The Angle with the vertical	ψ	Varies From -0.8722 rad To 0.8722 rad For every cycle
Radius of the C-Leg	r_1	0.1625 m

3.3 Results for the Quadruped Robot for the Bounding Gait

Bounding gait can be obtained by combining all the four phases i.e. Back Stance, Back Flight, Front Stance, Front Flight. To achieve running, bounding gait can be actuated repeatedly. Simulation is done by repeatedly running bounding gait for the prescribed time period i.e.10 seconds.
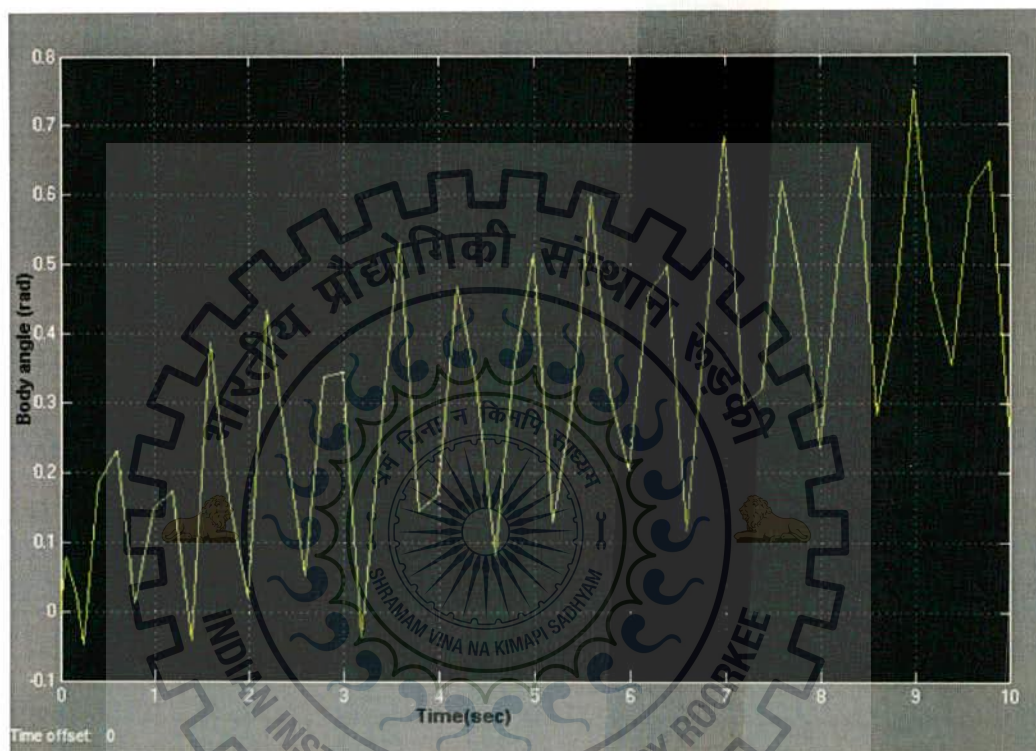

Figure 3: variation of body angle (θ) with respect to time

Fig 3.8 shows the variation of body angle (θ) with respect to time. Initially during back stance phases, it starts to rotate in counter clockwise direction whereas it is in clockwise in case of front stance phases. During flight phases, it reaches zero radian at first. But because of the inclination of the ground (θ_g) of 0.1 radian, it slowly increases on the positive side.
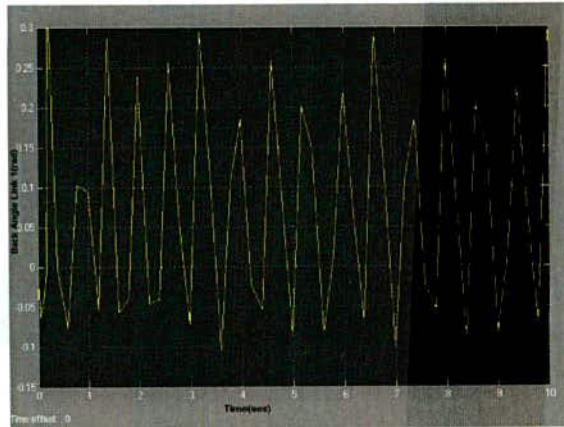
Figure 3.94: variation of back leg angle of link1 (θ1) w.r.t. time

Fig 3.9 shows the variation of back leg angle of link1 (θ_1) with respect to time. During back stance phases, torque is applied at link1 of back leg and it rotates in clock wise direction. For making the robot to lift-off, it is actuated to rotate in counter clock wise direction during front stance phases. During the flight phases, the motor is actuated to bring the angle of rotation to zero position.
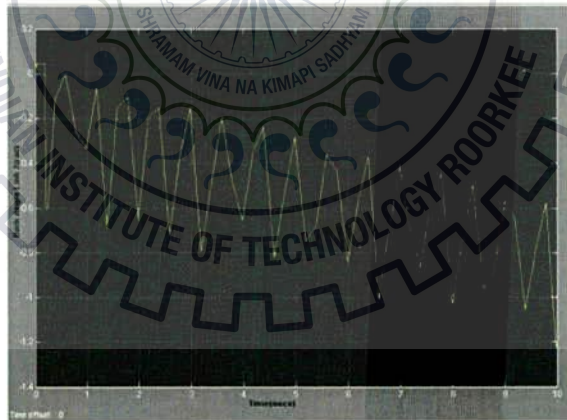

Figure 50: variation of C-link (θ2) of the back leg w.r.t. time

Fig 3.10 shows the variation of C-link (θ_2) of the back leg with respect to time. During back stance phases, torque is applied at C-link of back leg and it rotates in counter clock wise direction. For making the robot to lift-off, it is actuated to rotate in clock wise direction

during front stance phases. During the flight phases, the motor is actuated to bring it to zero position. But again due to the inclination it slowly decreases to the negative side.
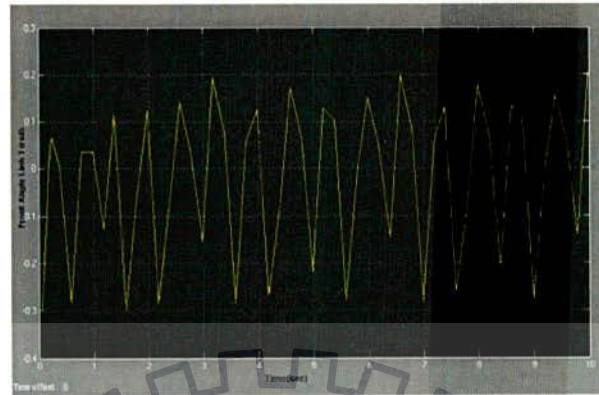

Figure 6: variation of front leg angle link1 (θ3) w.r.t. time

Fig 3.11 shows the variation of front leg angle of link1 (θ_3) with respect to time. For making the robot to lift-off, it is actuated to rotate in clock wise direction during back stance phases. During front stance phases, torque is applied at link1 of front leg and it rotates in counter clock wise direction. During the flight phases, the motor is actuated to bring it to zero position.
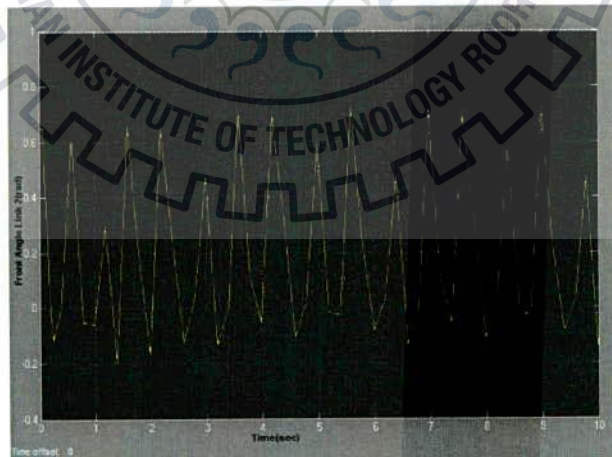

Figure 3.12: variation of C-link (θ4) of the front leg w.r.t. time

Fig 3.12 shows the variation of C-link (θ_2) of the back leg with respect to time. During back stance phases, torque is applied at C-link of back leg and it rotates in counter clock wise direction. For making the robot to lift-off, it is actuated to rotate in clock wise direction during front stance phases. During the flight phases, the motor is actuated to bring it to zero position. But again due to the inclination it the variation is increasing, but very slowly.

The X-Direction Variation of the body on an inclined plane

Figure 3.13:: Variation of the body in X-Direction

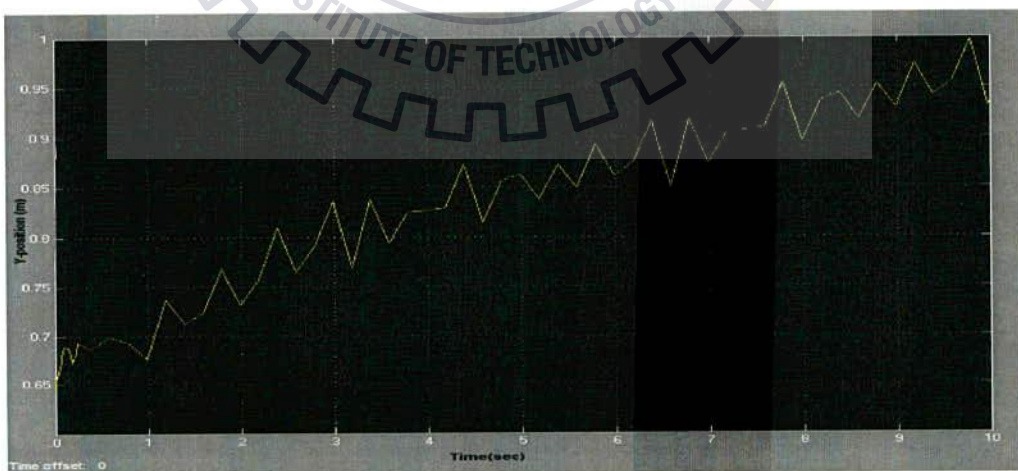**The Y-Direction Variation of the body on the inclined plane**

Figure 3.147: Variation of the body in Y-Direction

Fig 3.13 and 3.14 shows the variation movement of body position with respect to time. Back leg tip position has been taken as the reference axis and it is 0.4m in X direction and 0.65 in Y direction. During stance phases, the body prepares for the flight phases. It makes slight motion during stance phases in both the direction. Whereas it's motion is more during the flight phases. Fig 18

shows that the body transverse to 15 m in just 10 seconds. At the beginning position of body in Y direction is 0.65m. It moves up when the new phase starts afterwards it comes down and reaches the earlier values.

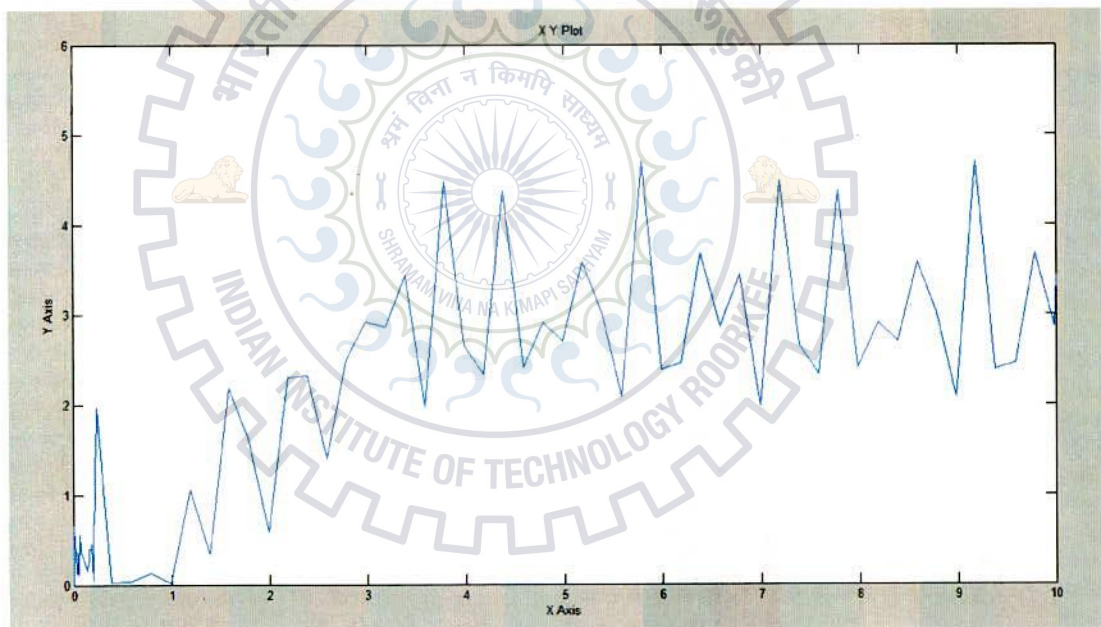**The X-Y Graph of the Bounding gait**


Figure 3.15: X-Y Graph of the Bounding gait

During the 10 seconds of the locomotion, the body moves in the bounding gait on an inclined plane. The above Fig. shows the Y-values for each X-value of the Body position of the four legged robot on an inclined plane with an inclination of 0.1 rad(approx. 5.7 degrees) during the 10 seconds.

CHAPTER 4   ANIMATION

Four legged walking robot with variable compliant C-leg (links) is animated by providing position and angle of rotation made by body and legs. All these parameters vary as the time progresses. The model in animated assuming it is on an inclination of 0.1 rad.

The four legged robot is animated using the SYMBOLS SHAKTI ANIMATOR. In order to transfer from MATLAB/Simulink to SYMBOLS, the X-co-ordinates and Y-co-ordinates of the all the joints and the centre of gravity of the robot are extracted from the Simulink model and then inserted in the SYMBOLS model of the robot to complete the animation.

The difficulties experienced during the animation in SYMBOLS is that the software did not have an option of the C-Leg(Link). Hence, here the C-leg(Link) is represented by a spring.

4.1 Snapshots

Robot at Rest

Back Stance   Back Flight   Front Stance   Front Flight
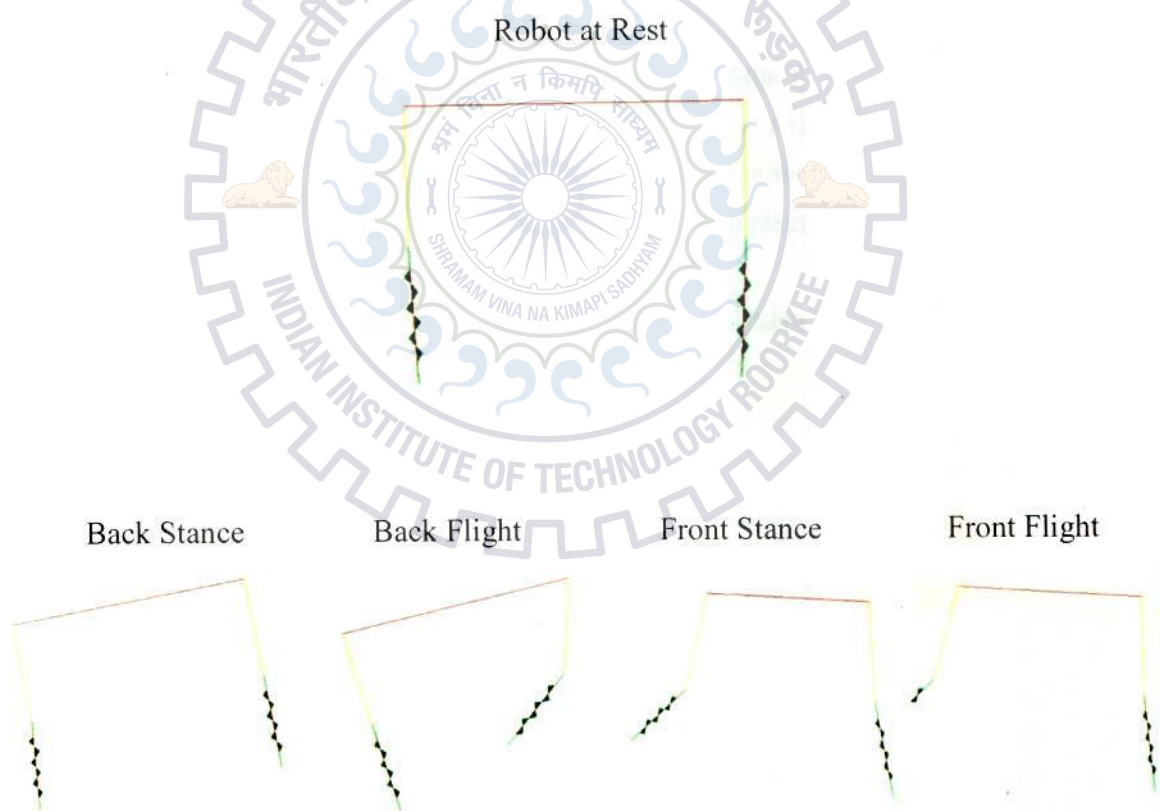
The snapshots of the robot running on an inclined plane are shown in the Fig. We can observe from this animation that the body's inclination in the back stance is more than the body's inclination in the front stance. From this it is clear that the robot is running on an inclined plane.

CHAPTER 4   CONCLUSION AND FUTURE SCOPE

4.1 Conclusion

This thesis report deals with the dynamic modelling of a four legged walking robot with variable compliant C-Leg(Links). Dynamic modelling was made for the four running phases of bounding gait by Lagrange-Euler method. Simulation was done with the assumed robot parameters. It was animated successfully and also gives the clear view of running cycle. .

Till now research work has not been started in four legged walking robot with variable complaint C-legs(Links) in which each legs are having two links. In dynamic modelling of the four legged robot's various factors such as masses of body and legs, friction, impact force and inclined ground surface have been considered.

4.2 Scope for future work

Even though the simulation and animation were successfully implemented in four legged walking robot with variable complaint C-legs (Links), there is some area for the future work.

a. Control algorithms for controlling the forward speed and the Trajectory of the robot can be designed to make the robot follow a specific path at a specific speed.

b. Experimental setup can be made for the parameters used in simulation by installing various sensors. Above dynamic modelling and can be implemented in that setup, if the control algorithm is available.

c. Experimental work for different control algorithms and dynamic models can be done for different gaits.

REFERENCES

1. H. Miura and I. Shimoyama. "Dynamic walk of a biped" International Journal of Robotics Research, 3(2), pages 60-74, Summer 1984.

2. M. H. Raibert. "Legged Robots That Balance" MIT Press, Cambridge, MA, 1986. [35] W.J. Schwind and D.E. Koditschek. Control of Forward Velocity for a Simplified Planar Hoping Robot. In Proc. IEEE Int. Conf. Robotics and Automation, pages 691-696, 1995.

3. T. McGeer. "Passive Bipedal Running" Simon Fraser University, Burnabay, BC, April 1989.

4. Y.Y. Keon. "Locomotion of a biped robot with compliant ankle joints" In Proc. IEEE Int. Conf. Robotics and Automation, vol.1, pages 199-204 , 1997.

5. H. Kimura, K. Sakurama and S. Akiyama "Dynamic Walking and Running of the Quadruped Using Neural Oscillator" IROS 1998.

6. J. Furusho, A. Sano, M. Sakaguchi, and E. Koizumi "Realization of Bounce Gait in a Quadruped Robot with Articular-Joint-Type Legs" In Proc. IEEE Int. Conf. Robotics and Automation, pages 697-702, May 1995.

7. M.D. Berkemeier "Approximate Return Maps for Quadrupedal Running. In Proc. IEEE Int. Conf. Robotics and Automation", pages 805-810, Albuquerque, New Mexico, April 1997.

8. Rafael Fontes Souto, Geovany Ara´ujo Borges and Alexandre Ricardo Soares Romariz "Gait generation for a quadruped robot using Kalman filter as optimizer" IEEE/RSJ International Conference on Intelligent Robots and Systems October 11-15, 2009

9. Mojtaba Ahmadi and Martin Buehler "Stable control of a Simulated One-Legged Running Robot with Hip and Leg Compliance" (1984)

10. Didier Papadopoulos and Martin Buehler "Stable Running in a Quadruped Robot with Compliant Legs" IEEE Int. Conf. Robotics and Automation, San Francisco, 2000

11. Nicholas Cherouvim and Evangelos Papadopoulos "Single Actuator Control Analysis of a Planar 3DOF Hopping Robot" (2003)

12. Evangelos Papadopoulos, Nicholas Cherouvim "On Increasing Energy Autonomy for a One-Legged Hopping Robot" Proceedings of the 2004 IEEE International Conference on Robotics & Automation April 2004

13. Umberto Scarfogliero , Cesare Stefanini , Paolo Dario "The use of compliant joints and elastic energy storage in bio-inspired legged robots" Mechanism and Machine Theory (2008)

14. Katayon Radkhah, Stefan Kurowski, and Oskar von Stryk "Design Considerations for a Biologically Inspired Compliant Four-Legged Robot" IEEE International Conference on Robotics and Biomimetics December 19 -23, 2009

15. E. Sayinger, Y. Yazicioglu, A. Saranli and u. Saranli "A Dynamic Model of Running with half Circular C-leg" WSPC Proceedings 2012

16. K. Ganesh and Dr. Pushparaj Mani Pathak "Modeling and Simulation of Four Legged Jumping Robot with Compliant Legs in sagittal plane" Robotics and Autonomous Systems 2011

17. Mittal R.K., Nagrath I.J., (2003) 'Robotics and Control' Tata McGraw-Hill Publishing Ltd., New Delhi, pp 190-239.

18. Spong W. Mark., Vidya Sagar M.,(2004) 'Robotics Dynamics and Control' John Wiley & Sons (Asia) pte Ltd., Noida, pp129-152.

19. Bansal R.K., Goel A.K., Sharma M.K., (2009) 'Matlab and its Applications in Engineering' Dorling Kindersley (India) Pvt Ltd., New Delhi, pp 230-262.

20. www.mathworks.com